Amorphous polymeric drug salts as ionic solid dispersion forms of ciprofloxacin

Hanah Mesallati[†], Anita Umerska[$], Krzysztof Paluch[§] and Lidia Tajber[*,†]

[†]Synthesis and Solid State Pharmaceutical Centre, School of Pharmacy and Pharmaceutical Sciences, Trinity College Dublin, College Green, Dublin 2, Ireland.

[$]MINT, UNIV Angers, INSERM 1066, CNRS 6021, Universite Bretagne Loire, 4 rue Larrey, Angers 49933 Cedex, France.

[§] School of Pharmacy and Medical Sciences, Faculty of Life Sciences, University of Bradford, Bradford, West Yorkshire, BD7 1DP, United Kingdom.

[*]School of Pharmacy and Pharmaceutical Sciences, Trinity College Dublin, College Green, Dublin 2, Ireland. Tel: +35318962787. Email: ltajber@tcd.ie.

Abstract

Ciprofloxacin (CIP) is a poorly soluble drug that also displays poor permeability. Attempts to improve the solubility of this drug to date have largely focused on the formation of crystalline salts and metal complexes. The aim of this study was to prepare amorphous solid dispersions (ASDs) by ball milling CIP with various polymers. Following examination of their solid state characteristics and physical stability, the solubility advantage of these ASDs was studied, and their permeability was investigated via parallel artificial membrane permeability assay (PAMPA). Finally, the minimum inhibitory concentration (MIC) and minimum bactericidal concentration (MBC) of the ASDs were compared to those of CIP. It was discovered that acidic polymers, such as Eudragit L100, Eudragit L100-55, Carbopol and HPMCAS, were necessary for the amorphization of CIP. In each case, the positively charged secondary amine of CIP was found to interact with carboxylate groups in the polymers, forming amorphous polymeric drug salts. Although the ASDs began to crystallize within days under accelerated stability conditions, they remained fully X-ray amorphous following exposure to 90% RH at 25 ^{o}C, and demonstrated higher than predicted glass transition temperatures. The solubility of CIP in water and simulated intestinal fluid was also increased by all of the ASDs studied. Unlike a number of other solubility enhancing formulations, the ASDs did not decrease the permeability of the drug. Similarly, no decrease in antibiotic efficacy was observed, and significant improvements in the MIC and MBC of CIP were obtained with ASDs containing HPMCAS-LG and HPMCAS-MG. Therefore, ASDs may be a viable alternative for formulating CIP with improved solubility, bioavailability and antimicrobial activity.

Keywords: ciprofloxacin, amorphous solid dispersion, polymer, polymeric drug salts, solubility, PAMPA.

Introduction

Ciprofloxacin (CIP) is a second generation fluoroquinolone antibiotic with a wide spectrum of activity. Anhydrous CIP usually exists as a zwitterion, as shown in Figure 1; however, it can convert to the unionized form when heated to approximately 270 ^{o}C or spray dried in a mixture of ethanol and water.[1] In solution, the carboxylic acid and piperazine of CIP can ionize, depending on the pH of the surrounding media. In the neutral pH range CIP is largely zwitterionic and has an overall neutral charge, making it practically insoluble in aqueous media. The solubility of CIP in water has been reported as 0.06 and 0.08 mg/mL at 25 ^{o}C and 37 ^{o}C respectively.[2] CIP is also poorly soluble in other common solvents such as ethanol, methanol, propanol, acetone and chloroform.[3] CIP is also known to display poor permeability, and therefore may be considered as a class IV Biopharmaceutics Classification System (BCS) drug.[4]

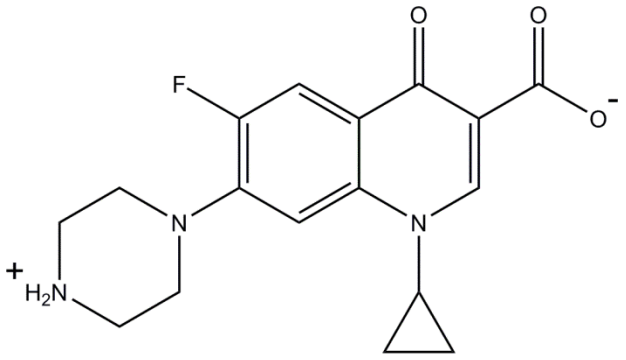

Figure 1. Structure of zwitterionic ciprofloxacin.

Due to the strength of its intermolecular interactions, the dissociation of CIP's crystal lattice upon addition to water is hindered. The solubility of the drug can therefore be improved by disrupting its crystal lattice via salt formation or amorphization.[5] Salt formation is the most frequently used process for improving the solubility of acidic and basic drugs, and is also

claimed to be the most effective.[6] For this reason it has been the main focus of research aimed at improving the solubility of CIP. The hydrochloride salt of CIP is available on the market as a tablet for oral administration. This form of the drug has been reported to have a solubility of approximately 42 mg/mL in water at 37 ^{o}C.[7] However, due to the common ion effect, the solubility of HCl salts is decreased in the stomach.[8] The lactate salt of CIP is available commercially as a solution for infusion, and has an aqueous solubility of just over 100 mg/mL.[9] Novel CIP salts have also been produced using malonic, tartaric and oxalic acid,[10] mesylic, gluconic and glycolic acid,[11] and saccharin.[12] All of these salts showed an improvement in solubility compared to the pure drug. As an alternative to small molecules, polymers may be used as counter ions in pharmaceutical salts. Willis et al found that the extent and rate of methapyrilene release in simulated gastric and intestinal fluid was improved by the formation of drug-polymer salts, in which the amine group of the drug and carboxyl groups of the polymer interacted.[13]

Another method for improving the aqueous solubility of drugs is amorphization. The amorphous form does not possess long range order, and is the most energetic solid state.[14] It is therefore more soluble than the crystalline form, as less energy is required to enter solution.[15] The production of amorphous and partially amorphous pure CIP by various techniques was recently described by our group. This was a challenging task, as the poor solubility and thermal degradation of CIP limit the techniques that can be used to amorphize it.[1]

A major disadvantage of amorphous formulations is that they are intrinsically unstable and prone to crystallization.[14] The most common approach taken to overcome the poor stability of amorphous drugs is to formulate them as amorphous solid dispersions (ASDs). ASDs consist of an amorphous dispersion of a drug in a solid carrier, where the carrier is either a small molecule

or polymer. The drug should ideally be molecularly dispersed.[16] The carrier used to form an ASD must be chosen carefully in order to maximize the stability and solubility of the product. The physical stability of an ASD is improved if there are interactions between the components, e.g. hydrogen bonding and acid-base interactions. This reduces the molecular mobility of the drug and increases the energy required for crystallization.[17] ASDs also enable faster drug dissolution, often resulting in supersaturation. The polymers present in an ASD help to prevent crystallization and precipitation of the drug in solution, and thus prolong this supersaturated state.[18]

Despite the benefits of amorphous formulations, there is very little information in the literature regarding the formation of CIP ASDs. However, the production of amorphous salts of CIP and succinic acid with a 1:1 and 2:1 stoichiometry has previously been described by Paluch et al. These salts increased the solubility of CIP in water at 37 ^{o}C by over 300 and 600 times respectively.[2] Other amorphous formulations of CIP which have been produced include nanoplexes formed using dextran sulfate,[19] and microparticles containing chitosan and dextran.[20]

Due to the lack of research in this area, the primary aim of this study was to prepare a number of solid dispersions of CIP with various polymers by ball milling, and to perform a comprehensive analysis of the successful ASDs. The solid state properties of the samples were first investigated, in particular the nature of their drug-polymer interactions and thermal stability. As previously mentioned, a major issue associated with amorphous formulations is their poor physical stability, however this can be counteracted to some degree by the use of polymers with high T_g's that interact specifically with the drug. The stability of the ASDs during dynamic vapor sorption (DVS) analysis and under accelerated conditions was therefore examined in order to determine their resistance to crystallization.

Another major goal of this study was to determine the effect of ASD formation on the biopharmaceutical properties of CIP, specifically its solubility, permeability and antimicrobial activity, and how these characteristics are connected. ASDs have been found to increase the solubility of drugs via supersaturation, while maintaining a constant permeability. In contrast, the solubility advantage obtained with formulations containing cyclodextrins, surfactants and cosolvents is negatively correlated with permeability.[21] The solubility of crystalline CIP and the ASDs was therefore investigated in water and biorelevant media, and their permeability was compared using parallel artificial membrane permeability assay (PAMPA), to discover whether a similar relationship exists between the solubility and permeability of these preparations. Finally, it was of interest to determine whether the formulation of CIP as an ASD affected its antimicrobial activity, which should also be related to permeability. Therefore, the minimum inhibitory concentration (MIC) and minimum bactericidal concentration (MBC) of CIP and the ASDs were measured in a number of bacterial species.

Materials and Methods

Materials

Anhydrous ciprofloxacin (CIP) was obtained from Carbosynth Limited, Berkshire, UK. Ciprofloxacin hydrochloride (CIP HCl) salt was kindly donated by Hemofarm, Serbia. The following polymers were used to form solid dispersions with CIP: Polyvinylpyrrolidone K17 (PVP, Plasdone® C-15, ISP Technologies, New Jersey, USA); polyvinylalcohol (PVA, 98% hydrolyzed, M_w 13000–23000, Sigma-Aldrich, St. Louis, Missouri); methacrylic acid methyl methacrylate copolymer (Eudragit® L100, Evonik Röhm GmbH, Darmstadt, Germany);

methacrylic acid ethyl acrylate copolymer (Eudragit® L100-55, Evonik Röhm GmbH, Darmstadt, Germany); poly(acrylic acid) (Carbopol® 981, BF Goodrich, Ohio, USA); hydroxypropyl methylcellulose acetate succinate grades LG and MG (HPMCAS-LG and HPMCAS-MG, Shin-Etsu Chemical Co., Ltd, Tokyo, Japan); polyvinyl caprolactam-polyvinyl acetate-polyethylene glycol graft copolymer (Soluplus®, BASF SE, Ludwigshafen, Germany); and polyethylene glycol 4000 (PEG 4000, BDH Ltd, Poole, England).

Fasted state simulated gastric fluid (FaSSGF) was produced by adding 60 mg SIF® Powder Original (biorelevant.com, Surrey, UK) to one liter of FaSSGF HCl solution, consisting of 34 mM NaCl adjusted to pH 1.6 with HCl. Fasted state simulated intestinal fluid (FaSSIF) was produced by adding 2.24 g SIF® Powder Original to one litre of FaSSIF phosphate buffer, consisting of 19.5 mM NaOH, 25 mM $NaH_2PO_4 \cdot H_2O$ and 106 mM NaCl, adjusted to pH 6.5 with NaOH. NaOH pellets were obtained from Riedel-de Haën®, Seelze, Germany, $NaH_2PO_4 \cdot H_2O$ from Merck, Darmstadt, Germany and NaCl from Sigma-Aldrich Ireland Ltd., Arklow, Ireland. Dodecane, triethylamine, lecithin (L-α-phosphatidylcholine, Type XVI-E) and phosphate buffered saline (PBS) tablets were obtained from Sigma-Aldrich Ireland Ltd., Arklow, Ireland. Brain-heart infusion (BHI) broth was purchased from bioMérieux (Marcy l'Étoile, France). Plates with Columbia agar supplemented with sheep blood were obtained from Oxoïd (Dardilly, France). All other chemicals and solvents were of analytical grade.

Methods

Ball Milling

CIP was first milled with PVP at a concentration of 10–95% (w/w). Solid dispersions of CIP with Eudragit® L100, Eudragit® L100-55, Carbopol® 981, HPMCAS-LG, HPMCAS-MG,

PVA, Soluplus® and PEG 4000 were also formed using 20–60% (w/w) polymer. For each sample, milling was performed at room temperature using a Retsch® planetary ball mill PM 100 (Haan, Germany). The only exception to this was the CIP/HPMCAS-LG and HPMCAS-MG ASDs, which were milled at 2–5 ^{o}C. 2 g of powder was added to 50 mL stainless steel grinding bowls. The three stainless steel milling balls were 20 mm in diameter and weighed 32 g each. The powder mixtures were each milled for 4–6 hours in total, in intervals of 15 min with 10 min breaks in between. At 1, 2, 4 and 6 hours, small samples of powder were taken for analysis by powder X-ray diffraction.

Powder X-ray Diffraction (PXRD)

PXRD was performed at room temperature using a benchtop Rigaku MiniflexII X-ray diffractometer (Tokyo, Japan) and a Haskris cooler (Illinois, USA). The measurements were carried out in reflectance mode. The samples were scanned from 5 to 40 2θ degrees in steps of 0.05. A scan rate of 0.05^{o} per second and signal collection time per step of 1 s were used. The tube (Cu, 1 kW normal focus) output voltage and current were 30 kV and 15 mA, respectively.

Solid State Fourier Transform Infrared Spectroscopy (FTIR)

FTIR was performed using a Spectrum One FT-IR Spectrometer (Perkin Elmer, Connecticut, USA) equipped with Spectrum Software version 6.1. A spectral range of 450–4000 cm^{-1}, resolution of 4 cm^{-1}, scan number of 10 and scan speed of 0.2 cm/s were used. KBr disks were produced by direct compression, using a pressure of approximately 10 bar for 1 min. A sample loading of 1% (w/w) was used. Physical mixtures (PMs), which were prepared by blending together the drug and polymers in the same ratio as in the ASDs with a mortar and pestle, were also analyzed for comparison.

Differential Scanning Calorimetry (DSC)

DSC was carried out using a Mettler Toledo DSC (Schwerzenbach, Switzerland). The purge gas was nitrogen. Approximately 5–10 mg samples were analyzed in sealed 40 µL aluminum pans with pierced lids. The ASDs were first heated from 25 to 70–100 ^{o}C to remove any water present in the powder. When cool, the samples were reheated from 25 to 300 ^{o}C at a rate of 10 ^{o}C/min. Mettler Toledo STARe software (version 6.10) was used to analyze the thermograms.

Temperature-Modulated Differential Scanning Calorimetry (StepScan™)

A PerkinElmer Diamond DSC (Waltham, MA, USA) and ULSP B.V. 130 cooling system (Ede, Netherlands) were used to detect the T_g's of the ASDs. A nitrogen gas flow of 40 mL/min was controlled with a PerkinElmer Thermal Analysis Gas Station. The instrument was calibrated for temperature and heat flow using indium standards. Approximately 5 mg samples were analyzed in 18 µL aluminum pans with sealed lids. Samples were heated at 5 ^{o}C/min in steps of 2 ^{o}C. Between each step the temperature was held constant for 1 min. The specific heat of the glass transition was calculated from the enthalpy flow using the area algorithm.

Calculation of Theoretical Glass Transition (T_g) Values with Gordon-Taylor Equation

The theoretical T_g's of the ASDs were calculated using the Gordon-Taylor equation:[22,23]

$$T_g = \frac{w_1 T_{g1} + K w_2 T_{g2}}{w_1 + K w_2} \quad (1)$$

where K is approximately equal to

$$K \approx \frac{T_{g1}\rho_1}{T_{g2}\rho_2} \quad (2)$$

w_1 and w_2 are the weight fractions, T_{g1} and T_{g2} are the glass transition temperatures, and ρ_1 and ρ_2 are the densities of the two components. The T_g of pure amorphous CIP was previously determined as 86.7 °C,[1] while the T_g's of the polymers were obtained from literature: Eudragit L100, 130 °C;[24] Eudragit L100-55, 96 °C;[25] HPMCAS-LG, 119 °C;[26] and HPMCAS-MG, 120 °C.[26] The average density values for the various components were also obtained from literature: CIP, 1.5 g/cm^3;[1] Eudragit L100, 0.84 g/cm^3;[27] Eudragit L100-55, 0.83 g/cm^3;[28] and HPMCAS-LG and HPMCAS-MG, 1.29 g/cm^3.[29] The T_g's predicted by the Gordon-Taylor equation were then compared to the experimental values measured by DSC.

Thermogravimetric Analysis (TGA)

TGA was carried out on the ASDs using a Mettler TG50 measuring module coupled to a Mettler Toledo MT5 balance (Schwerzenbach, Switzerland). Approximately 8–10 mg samples were analyzed in open aluminum pans, using nitrogen as the purge gas. Samples were heated from 25 to 300 °C at a rate of 10 °C/min. Mettler Toledo STARe software (version 6.10) was used to analyze the thermograms.

Dynamic Vapor Sorption (DVS)

DVS studies were carried out using an Advantage-1 automated gravimetric vapor sorption analyzer (Surface Measurement Systems Ltd., London, UK). The temperature was maintained at 25.0 ± 0.1 °C. Approximately 10 mg of ASD was added to the sample basket and placed in the instrument. The samples were equilibrated at 0% relative humidity (RH) until a constant mass was obtained (dm/dt ≤ 0.002 mg/min). The reference mass was recorded and sorption-desorption analysis was then carried out between 0 and 90% RH, in steps of 10% RH. At each stage, the sample mass was equilibrated (dm/dt ≤ 0.002 mg/min for at least 10 min) before the RH was

changed. An isotherm was calculated from the complete sorption and desorption profile. Following DVS analysis the samples were analyzed by PXRD in order to detect any crystallization.

Accelerated Stability Study

A stability study of the ASDs was conducted under accelerated storage conditions of 40 ^{o}C and 75% RH. Samples of each powder were taken every 2–3 days for a period of 2 weeks. PXRD was used to determine whether crystallization had occurred in any of the samples.

Dynamic Solubility Studies

10–20 mL of water, FaSSIF or FaSSGF was added to 40 mL glass vials. These were placed into jacketed beakers connected to a Lauda M12 water bath (Lauda-Königshofen, Germany) and allowed to equilibrate to 37 ^{o}C. A quantity of pure drug or ASD, in excess of the expected saturated solubility (50–225 mg, depending on the sample), was added to the stirred vials. Samples were drawn from the vials at specific time points over a 2 hour period. These aliquots were filtered with 0.45 μm PTFE membrane filters (VWR, USA). The filtered solutions were then diluted with a 2.45 g/L solution of phosphoric acid, previously adjusted to pH 3.0 with triethylamine. The concentration of CIP in each of the diluted samples was determined by UV spectrophotometry. The solubility studies were repeated at least in triplicate with each medium. The pH of the solutions was measured before the addition of the samples and at the end of the 2 hour study using a Thermo Orion 420A+ pH meter (Thermo Scientific, Hampshire, UK). The solid material left in the vials at the end of the studies was filtered and analyzed by PXRD.

UV Spectrophotometry

UV analysis was carried out using a Shimadzu UV-1700 PharmaSpec UV-vis spectrophotometer (Shimadzu Corp., Kyoto, Japan). Quartz cells with a 1 cm optical path length were used for all measurements. UV absorbance was measured at 278 nm. The instrument was first blanked using a 2.45 g/L solution of phosphoric acid, previously adjusted to pH 3.0 with triethylamine. This buffer was also used to produce a range of concentrations of pure CIP, in order to construct a calibration curve.

Parallel Artificial Membrane Permeability Assay (PAMPA)

Permeability studies were carried out using the Lipid-PAMPA method described by Merck Millipore.[30] A 96-well MultiScreen Filter Plate (Millipore Corporation, Billerica, MA, USA), with underdrain removed, was used as the donor plate, and a 96-well MultiScreen Transport Receiver Plate (Millipore Corporation, Billerica, MA, USA) as the acceptor plate. Solutions of CIP, CIP HCl, CIP/Eudragit L100, CIP/HPMCAS-LG and CIP/HPMCAS-MG in PBS pH 7.4 and 6.4, at concentrations of 50–125 μg/mL, were prepared. 300 μL of PBS pH 7.4 was added to each well of the acceptor plate. 5 μL of a 1% (w/v) solution of lecithin in dodecane was added to the filter within each donor well to form an artificial membrane. 150 μL of the drug solutions were immediately added to each well of the donor plate in triplicate. The donor plate was then placed into the acceptor plate and incubated at room temperature for 16 hours. Following incubation, the contents of each well in the acceptor plate was diluted 1:4 with HPLC mobile phase and filtered with 0.45 μm PTFE membrane filters (VWR, USA). The concentration of CIP in each sample was then measured using HPLC.

The effective permeability (P_e) of the samples was calculated using the following equation reported by Wohnsland and Faller:[31]

$$P_e = -\ln(1 - r)\left(\frac{V_D V_A}{(V_D+V_A)At}\right) \text{ where } r = \frac{[Drug]_{Acceptor}}{[Drug]_{Equilibrium}} \quad (3)$$

V_D and V_A are the volumes of the donor and acceptor compartment, respectively, in cm^3, t is the incubation time in seconds, and A is the active surface area of the membrane (equal to the membrane area multiplied by the porosity ratio. For Millipore MultiScreen Permeability Filter Plate membranes this is equal to 0.24 cm^2 x 100%, or 0.24 cm^2).[30] $[Drug]_{Acceptor}$ is the concentration of the drug in the acceptor compartment at the end of the assay. $[Drug]_{Equilibrium}$ is determined by measuring the concentration of a reference solution, containing the drug at the theoretical equilibrium concentration (the overall concentration of the donor and acceptor solutions combined).[32] Given that the acceptor and donor compartments used in this study had a volume of 150 µL and 300 µL respectively, the equilibrium concentration of the drug should theoretically be one-third of that of the original solution added to the donor well.

High Performance Liquid Chromatography (HPLC)

The content of CIP was measured with a Shimadzu® 10Avp HPLC system (Kyoto, Japan). A Luna 5u C8 column, with a length of 250 mm, internal diameter of 4.6 mm and 5 µm particle size, was used. The mobile phase consisted of 13 volumes of acetonitrile and 87 volumes of a 2.45 g/L solution of phosphoric acid, previously adjusted to pH 3.0 with triethylamine. An injection volume of 10 µL and flow rate of 1.5 mL/min for 15 min was used. The separation was carried out at room temperature. A Shimadzu SPD-10Avp UV-vis Detector at 278 nm was used to detect the drug.

Bacterial Studies

Bacterial studies were carried out on the following bacterial strains: (1) *Staphylococcus aureus* ATCC 25923, (2) *Escherichia coli* ATCC 25922, (3) *Pseudomonas aeruginosa* ATCC 27853 and (4) *Klebsiella pneumoniae* DSM 16609. The bacteria were cultured on Columbia agar supplemented with sheep blood. The inoculum was prepared as described previously.[33] The density of the microorganism suspension was adjusted to equal that of the 1.1 McFarland standard for *S. aureus*, and the 0.5 McFarland standard for *P. aeruginosa*, *E. coli* and *K. pneumoniae*. The former suspension was further diluted 100-fold with BHI medium, while the latter were diluted 10-fold.

The Minimum Inhibitory Concentrations (MICs) of CIP and the ASDs were determined using the broth microdilution method described by Umerska et al.[33] Several two-fold dilutions of the samples in BHI medium were prepared in order to obtain the desired concentration range. 50 µL of the bacterial suspension in BHI broth was then added to a well containing 50 µL of test sample or a control. The samples were incubated for 24 hours at 37 °C. All MIC assays were performed in triplicate on separate days. The MIC was taken to be the lowest concentration that completely inhibited the growth of bacteria, as detected by the unaided eye. The Minimum Bactericidal Concentrations (MBCs) were determined by withdrawing 10 µL from each well, transferring it onto a plate containing Mueller Hinton agar, and incubating overnight at 37 °C. MIC and/or MBC values were considered as different if they varied by more than one dilution.[33]

Statistical Analysis

Statistical analysis was carried out using Minitab® 16 software. Data was analyzed using analysis of variance (ANOVA) with Tukey's multiple comparison test, and two-sample Student *t* tests. A *p*-value of ≤ 0.05 was considered significant.

Results and Discussion

Production of Amorphous Solid Dispersions

A number of binary solid dispersions of CIP with different polymers, in various concentrations, were produced by ball milling. Ball milling was previously found to be a suitable method for forming the amorphous CIP/succinic acid 2:1 salt, as it did not result in any degradation of the drug.[2] The first polymer to be used was PVP, in a concentration range of 10–95% (w/w). PVP was chosen as it is a neutral, amorphous polymer, which is commonly used to produce ASDs of poorly soluble drugs.[16] Interestingly, CIP did not become amorphous when milled with any concentration of PVP tested. As the ratio of polymer to drug increased, the intensity of the peaks seen in the PXRDs decreased (Figure SI.1). However, this was most likely due to a dilution effect. Although CIP may theoretically interact with PVP via hydrogen bonds, these interactions were evidently too weak to yield a fully amorphous solid dispersion. Similarly, when CIP was milled with 40% (w/w) Soluplus or PEG 4000, both neutral polymers, a crystalline product was obtained (Figure 2a).

The next polymer chosen for milling with CIP was polyvinyl alcohol (PVA), whose hydroxyl group can act as both a hydrogen bond acceptor and donor. Following 4 hours of milling at room temperature with 40% (w/w) PVA, small peaks were still seen by PXRD (Figure 2a). Milling at room temperature can result in increased temperatures, and a subsequent increase in molecular mobility.[34] This can induce nucleation and crystallization of amorphous material. The use of too low a concentration of polymer can also result in an unstable product.[35] Therefore, a higher concentration of 60% (w/w) PVA, 6 hour milling time and milling temperature of 2–5 ^{o}C were

implemented. This resulted in a product which was almost fully amorphous, however very small peaks could still be detected at approximately 20 and 25 2θ degrees due to the presence of residual crystalline CIP (Figure SI.2).

As polymers with neutral functional groups were ineffective at amorphizing CIP, it was hypothesized that perhaps a polymer with ionizable moieties is necessary for this. As discussed above, many salts of CIP have been produced using acidic counter ions, such as succinic acid. The secondary amine of CIP's piperazine ring is ionized in these salts, and forms hydrogen bonds with the negatively charged carboxylate groups of the acid.[2] Therefore, the processing of CIP with acidic polymers may be a suitable means of producing a stable amorphous formulation. Eudragit L100, Eudragit L100-55 and Carbopol 981 all contain carboxylic acid groups, and were the first acidic polymers to be used. As can be seen from Figure 2b, each of these polymers resulted in the formation of an X-ray amorphous solid dispersion when milled with CIP for 4 hours at room temperature, at a concentration of 40% (w/w). While higher ratios of polymer were also successful, the use of lower quantities of the Eudragit polymers resulted in a partially crystalline product (Figure SI.3). Carbopol on the other hand still produced an ASD when used at a concentration of 20% (w/w).

HPMCAS also contains acidic groups. The LG grade contains 5–9% acetyl and 14–18% succinoyl groups, and the MG grade 7–11% and 10–14% of each group respectively.[26] However, when these were milled with CIP using the same conditions as for the other acidic polymers, the product was only partially amorphous (Figure 2a). Higher concentrations of polymer and longer milling times still resulted in partially crystalline systems, as evidenced by PXRD peaks, although polymer concentration appears to have a greater effect on the crystallinity of these samples than milling time (Figure SI.4). Milling was next conducted at 2–5 ^{o}C, with a 60 %

(w/w) concentration of HPMCAS, for 6 hours. These conditions resulted in the formation of X-ray amorphous solid dispersions (Figure 2b).

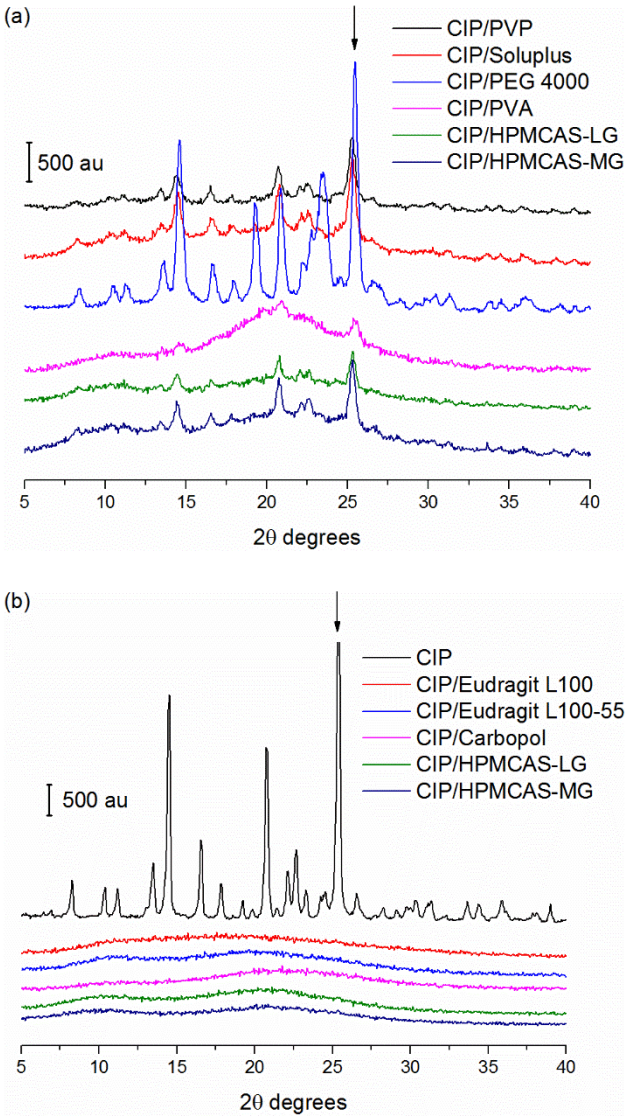

Figure 2. (a) PXRD analysis following milling of CIP with various polymers at a 40% (w/w) concentration, for 4 hours at room temperature. (b) PXRD analysis of CIP and CIP ASDs. The peak at 25.3 2θ degrees corresponds to the major slip plane in the crystal lattice of CIP, and therefore it is the most likely peak to be present following mechanical stress of the drug.[1]

ASDs formed from the five acidic polymers discussed above (i.e. Eudragit L100, Eudragit L100-55, Carbopol 981, HPMCAS-LG and HPMCAS-MG) were chosen for further examination. While a higher proportion of polymer should increase the physical stability of an ASD,[36] it also necessitates the use of a larger preparation in order to deliver the required dose as an oral solid dosage form. This could result in problems with patient acceptability and compliance. Therefore, a polymer concentration of 40% (w/w) was chosen for the ASDs containing Eudragit L100, Eudragit L100-55 and Carbopol, and 60% (w/w) for those containing HPMCAS.

Solid State Characterization of Amorphous Solid Dispersions

The FTIR spectra of the ASDs, polymers and crystalline CIP are shown in Figure 3. The spectra of the physical mixtures (PMs) are also shown for comparison.

In the spectra of each of the polymers, a peak can be seen between 1709 and 1744 cm^{-1} due to the C=O stretch of their carboxylic acid groups. A matching peak is present in the spectra of the PMs. The spectrum of crystalline CIP contains a peak at 1590 and 1375 cm^{-1}, corresponding to the asymmetric and symmetric vibrations of the carboxylate ion, respectively.[37] The peak at 1590 cm^{-1} is absent from the spectra of the ASDs containing Eudragit and Carbopol, while those containing HPMCAS display a small peak, due to the presence of a residual amount of zwitterionic CIP. Interestingly, with all of the ASDs a strong peak is seen between 1723 and 1734 cm^{-1}, due to the C=O stretch of COOH. In each case, this peak is far more intense than the corresponding peak in the spectra of the PMs. Therefore, these peaks can be assigned to the carboxylic acid of CIP, and it can be concluded that this group is uncharged in the ASDs. This is in contrast to the semi crystalline solid dispersions containing PVP and Soluplus, which also show the characteristic peaks of the ionized carboxylate group of CIP. These peaks are weaker

and broader in the more disordered CIP/PVA solid dispersion, as the proportion of crystalline CIP is greatly reduced. In addition, like the ASDs, this sample has a peak at approximately 1720 cm^{-1}, which confirms the presence of the protonated carboxylic acid group of CIP (Figure SI.5).

The strongest peak in the spectrum of crystalline CIP, at approximately 1618 cm^{-1}, can be assigned to the C=O stretch of the ketone carbonyl.[37] This peak is shifted to 1628 cm^{-1} in the spectra of the ASDs, which may be due to changes in the hydrogen bonding of this group. This peak was also found to shift to 1627–1629 cm^{-1} when zwitterionic CIP was heated to its melting point, which results in the formation of the unionized form of the drug.[1] When the carboxylic acid of CIP is unionized, an intramolecular hydrogen bond is formed between this ketone and the neighboring carboxylic acid.[1] This hydrogen bond is also found in CIP salts, in which the carboxylic acid of CIP is also protonated.[2] In contrast, no such shift in the ketone carbonyl peak is seen in the spectra of the semi-crystalline solid dispersions, as they contain zwitterionic CIP.

In each of the ASD spectra a broad peak at 2400–2600 cm^{-1} can be assigned to the NH_2^+ stretching vibrations of CIP.[2] Therefore, the drug is in a similar ionization state in these ASDs as it is in crystalline salts formed using various acids, i.e. with a neutral carboxylic acid and positively charged secondary amine. This group most likely interacts with negatively charged carboxylate groups in the polymers, as was seen with CIP succinate salts.[2] The pK_a of the carboxylic acid of CIP has been reported as 6.16, while that of the piperazine amine is 8.62.[38] Given that the pK_a values of the polymers vary from 5 to 6.0,[24–26,39] the pK_a difference between the secondary amine of the drug and carboxylic acid of the polymers falls within the limits of salt formation of $\geq$ 2–3 in each case.[40] Therefore, these formulations could be considered as amorphous polymeric drug salts. Amorphous drug-polymer salts have also been produced by

Weuts et al,[41] Song et al[42] and Maniruzzaman et al.[43] In each case an ionic interaction between the COOH groups of the polymers and amino groups of the drugs was detected.

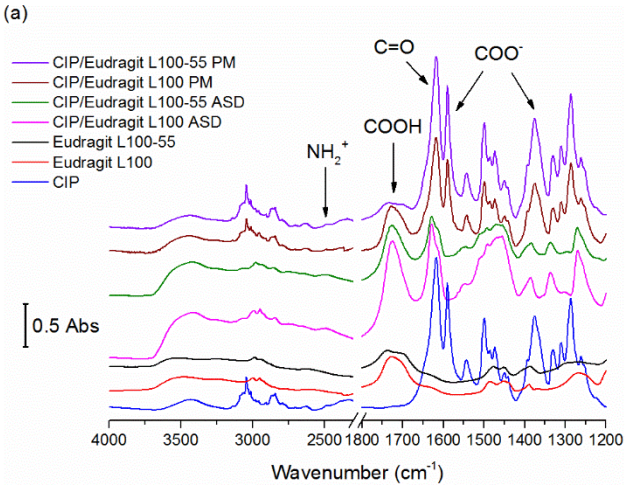

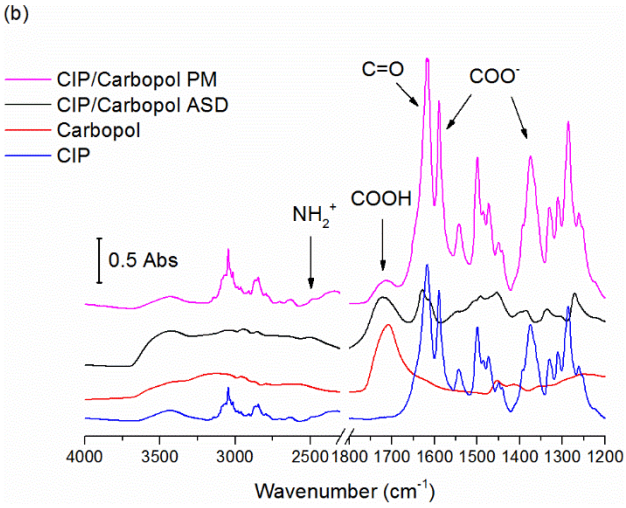

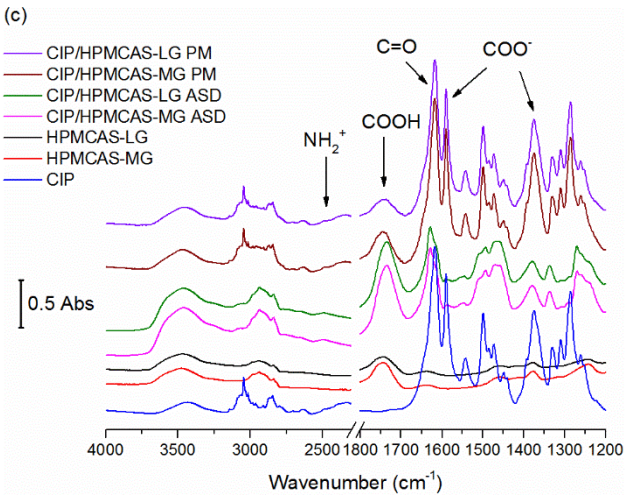

Figure 3. FTIR spectra of ASDs and PMs containing (a) Eudragit L100 and Eudragit L100-55 40% (w/w) (b) Carbopol 40% (w/w) and (c) HPMCAS-LG and HPMCAS-MG 60% (w/w).

Conventional DSC, using a heating rate of 10 ºC/min, resulted in DSC thermograms that proved difficult to interpret for these samples (Figure 4a). In each case it was impossible to pinpoint a definite glass transition temperature (T_g). Due to their high water content, the samples were first heated from 25–100 ºC to allow for evaporation of sorbed water.

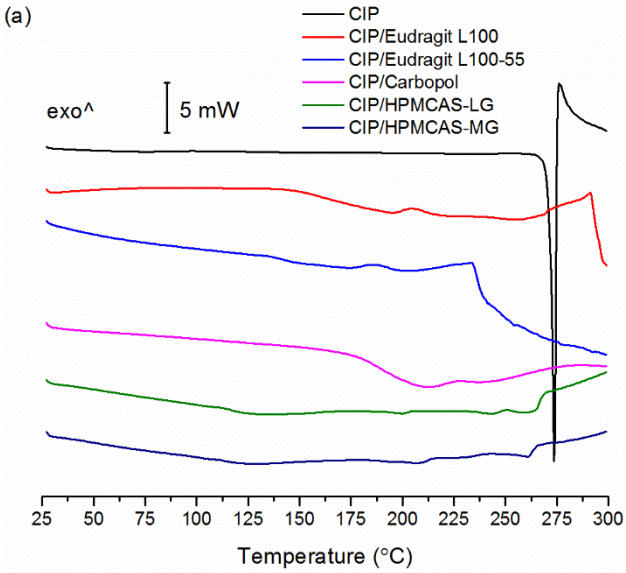

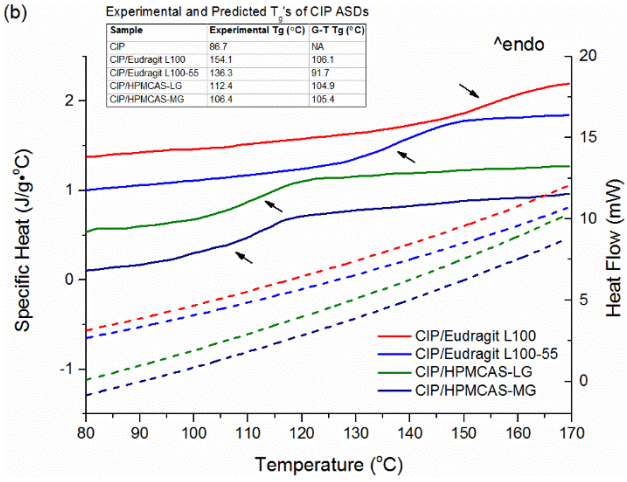

Figure 4. (a) Conventional DSC thermograms of CIP and CIP ASDs. The thermograms of the ASDs are those obtained from the second heating cycle, following initial heating to 100 ^{o}C to allow for water evaporation. (b) Heat flow traces from temperature modulated DSC (StepScan). Solid lines: specific heat curves; dotted lines: isokinetic baseline curves. The arrows point to the location of the T_g's. The T_g's obtained using the StepScan method as well as those calculated using the Gordon-Taylor (G-T) equation are also listed.

Crystalline CIP has a melting point of approximately 272 ^{o}C, which is accompanied by degradation. The ASDs did not display a clear melting endotherm, which can be taken as confirmation of their amorphous nature.[44] Like the pure drug, the ASDs undergo thermal degradation, as shown by TGA (Figure SI.6). All of the ASDs initially underwent water evaporation, followed by substantial degradation above ~ 230 ^{o}C, leading to a total mass loss of 14–19%.

Temperature-Modulated DSC (StepScan) was used to locate the T_g's of the ASDs, and these are listed in Figure 4b. No crystallization in the temperature range 80–170 C was detected using the StepScan method, as can be seen from the isokinetic baseline traces (Figure 4b). A single T_g was visible in the thermograms of all of the ASDs. This suggests that CIP is miscible with each of these polymers[45] and that phase separation does not occur in the ASDs.[15] Unfortunately, despite the use of the StepScan method, the T_g of the CIP/Carbopol ASD could not be detected. The T_g's that were calculated using the Gordon-Taylor (G-T) equation are also shown in Figure 4b. The G-T equation is based on the assumption that the components form an ideal mixture, with additive free volumes, but without any strong interactions between the constituents.[22,23] For all of the ASDs the T_g values obtained experimentally were higher than those predicted theoretically. This was also found to be the case for the amorphous polymeric salts produced by Weuts et al

and Song et al.[41,42] Particularly large positive deviations of approximately 48 and 45 ºC were obtained for the ASDs containing Eudragit L100 and L100-55, respectively. The G-T equation is known to underestimate the T_g of salts due to their ionic bonds, and larger deviations are obtained with counterions that form stronger electrostatic interactions with the drug.[46,47] Therefore, the FTIR analysis and the higher than predicted T_g's of these ASDs suggest that ionic interactions exist between CIP and the polymers.

In contrast to the Eudragit-containing ASDs, the experimental and calculated T_g's of the CIP/HPMCAS-MG ASD were very similar, differing by only 1 ºC. This suggests that the drug and polymer are fully miscible and do not interact specifically with one another.[48] Alternatively, the strength of the interactions formed between the drug and polymer may be equal in strength to the homomolecular interactions in the pure components.[49] This formulation would therefore be expected to be less stable than the ASDs containing Eudragit L100 or L100-55. A larger deviation of 7.5 ºC was seen with CIP/HPMCAS-LG, suggesting that the drug interacts more substantially with this grade of HPMCAS, but less so than with the Eudragit polymers, possibly due to a larger content of succinoyl groups in this grade of HPMCAS. Similarly, stronger drug-polymer interactions may exist in the Eudragit-containing ASDs due to the higher proportion of carboxylic acid groups present in these polymers in comparison to HPMCAS (see polymer structures in Figure SI.7). This may explain why it was more difficult to amorphize the CIP/HPMCAS mixtures, with larger polymer concentrations, longer milling times and lower temperatures being required compared to the other ASDs.

Stability Studies

DVS analysis showed that all of the ASDs are capable of sorbing a large amount of water. At 90% RH, a change in mass of between 16 and 20% was seen for all of the samples. CIP/Eudragit L100 sample sorbed the greatest amount of water, and CIP/HPMCAS-MG the least. The sorption-desorption isotherms obtained with all of the samples had a similar sigmoidal shape and hysteresis (Figure 5). These results are to be expected, as amorphous drugs are more hygroscopic than their crystalline forms. Water can absorb into the internal structure of amorphous materials rather than just adsorb to the surface.[50] The presence of hygroscopic polymers would also have contributed to the water uptake of the ASDs.

Water sorption can negatively affect drug stability by increasing the rate of crystallization. This is due to a lowering of the T_g, increase in molecular mobility and plasticization by moisture.[50] However, all of the ASDs studied here remained amorphous following DVS analysis, as shown by PXRD (Figure SI.8). Electrostatic forces between the amino group of CIP and carboxylic acid of the polymers most likely stabilized the ASDs and prevented their crystallization during the study. Similar interactions were responsible for the improved stability of loperamide-polyacrylic acid and lapatinib-hydroxypropylmethylcellulose phthalate ASDs during stability studies.[41,42] In addition, the long chains of polymers can delay crystallization by sterically hindering the diffusion of drug molecules, blocking sites of crystal growth, and increasing the kinetic barrier to nucleation.[36,49]

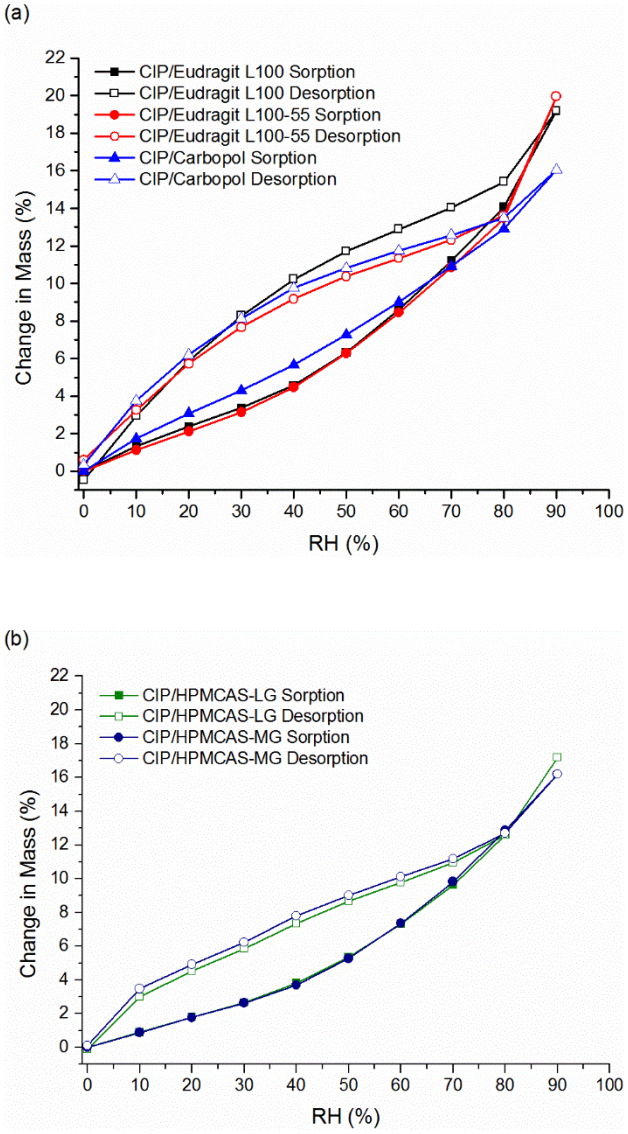

Figure 5. DVS analysis of CIP ASDs containing (a) Eudragit L100, Eudragit L100-55 and Carbopol 40% (w/w) and (b) HPMCAS-LG and HPMCAS-MG 60% (w/w).

All of the ASDs, except for CIP/Eudragit L100, began to crystallize after 24 hours in accelerated storage conditions of 40 ºC/75% RH. However, by day 3 of the study, this sample also began to show small crystallization peaks (Figure 6a). There was only a slight increase in the intensity of the bands seen in the PXRD of the HPMCAS samples between day 1 and 14, and no noticeable change in the Carbopol sample during the same timeframe (Figures 6b and c). As CIP/Eudragit

L100 did not show prominent peaks until day 3 of the study, it is therefore slightly more resistant to crystallization than the other ASDs. After 14 days, all of the samples were partially crystalline by PXRD, displaying a number of low intensity peaks. Therefore, although the ASDs were physically stable under the high humidity conditions of DVS, when this was combined with high temperature, a small degree of crystallization occurred. All of the ASDs, except for CIP/Carbopol, showed PXRD peaks corresponding to that of hydrated CIP, in particular the most characteristic peak of the 3.7 hydrate at approximately 6.5 2θ degrees.[51] Peaks corresponding to the 3.1 hydrate (see next section) were also identified. In contrast to the other ASDs, the peaks of hydrated CIP were absent from the diffractograms of the CIP/Carbopol ASD, which instead showed broad peaks corresponding to anhydrous zwitterionic CIP.

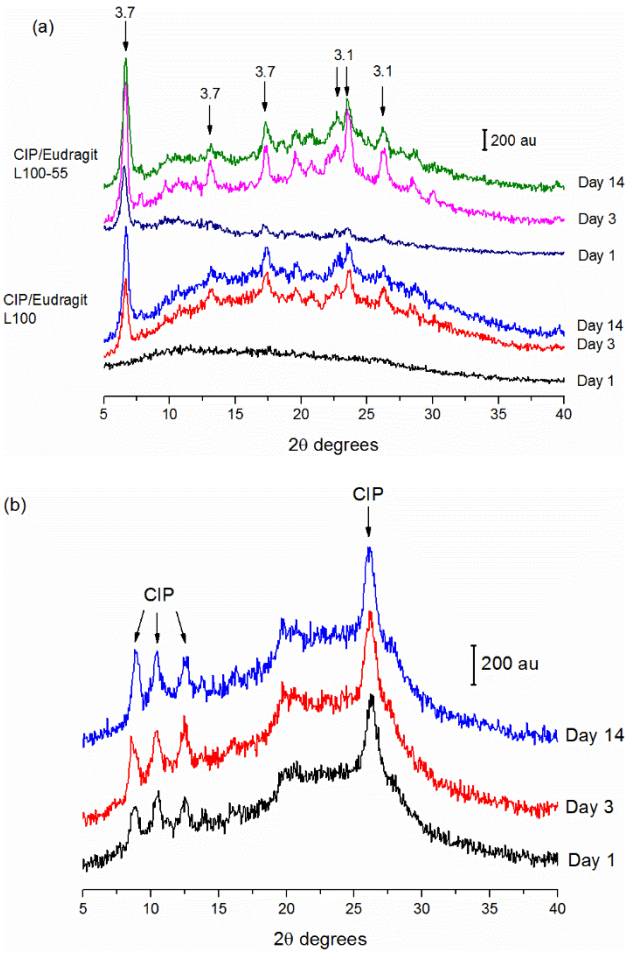

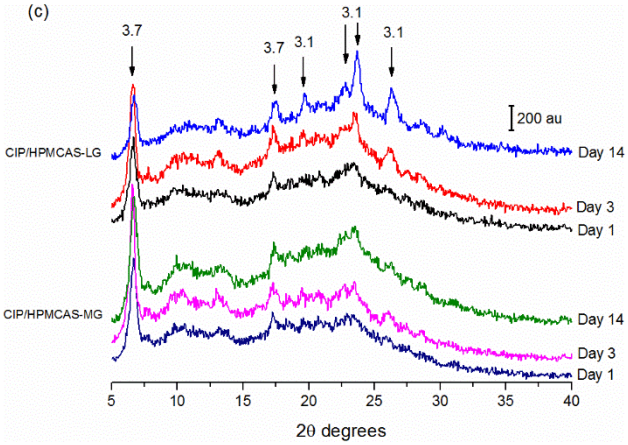

Figure 6. PXRD analysis of ASDs stored at 40 ºC/75% RH for 1, 3 and 14 days: (a) CIP/Eudragit L100 and CIP/Eudragit L100-55 (b) CIP/Carbopol and (c) CIP/HPMCAS-LG and CIP/HPMCAS-MG. The arrows identify the most prominent peaks, corresponding to CIP, CIP 3.7 hydrate (3.7) and CIP 3.1 hydrate (3.1).

Dynamic Solubility Studies

As previously mentioned, CIP is a zwitterionic compound, with a basic and an acidic group that can ionize depending on the pH of the solvent. Therefore, it is important to study the solubility of this drug in different media in order to estimate how it will behave in various sections of the gastrointestinal tract.[52] Solubility studies were carried out in water, FaSSIF (fasted state simulated intestinal fluid, pH 6.5) and FaSSGF (fasted state simulated gastric fluid, pH 1.6). Due to excessive clumping and the viscous nature of the solutions formed when the CIP/Eudragit L100-55 and Carbopol samples were added to the media, it was not possible to accurately carry out solubility tests on these ASDs.

CIP has low aqueous solubility, achieving a concentration of only 0.09 mg/mL in water after 2 hours. The Eudragit and HPMCAS ASDs showed superior solubility, obtaining concentrations approximately 7 and 19 times that of the pure drug, respectively, in the same time frame. After a

steep initial increase in concentration within the first 10 minutes or so, these levels were then sustained for the duration of the experiment (Figure 7a). All three of these polymers are practically insoluble in water,[26,27] which may have limited their ability to improve the aqueous solubility of CIP. Although the LG grade of HPMCAS resulted in slightly higher drug concentrations in the initial portion of the study, after 2 hours no statistically significant difference was seen when compared to the MG grade ($p = 0.27$).

The solubility profiles of the ASDs are similar to the "spring" and "parachute" model described by Guzmán et al.[18] Due to their disordered structure, ASDs enable the rapid dissolution of drugs and act as a "spring" for the formation of a supersaturated solution. Unfortunately, the high energy supersaturated state is usually short-lived, and amorphous drugs tend to quickly convert to more a stable and less soluble crystal form. This leads to precipitation of the API and reduced absorption in vivo. However, polymers which are present in the ASD can inhibit the nucleation and crystallization of the drug, decreasing the rate of precipitation.[53] In this way they act as "parachutes", helping to maintain supersaturation, and thus increase the rate and extent of drug absorption.[18] The polymers present in the CIP ASDs appear to have played a similar role, enabling high concentrations of CIP to remain in solution for at least 2 hours.

PXRD analysis of the excess solid recovered at the end of the studies confirms that a low proportion of CIP crystallized from the ASDs in solution overall (Figure SI.9). CIP/Eudragit L100 was quite resistant to crystallization in water, with just one small peak appearing in the PXRD of the excess solid recovered at the end of the study, at 6.5 2θ degrees. The HPMCAS ASDs showed a greater number of peaks, of higher intensity, but still remained somewhat disordered. As demonstrated in the stability study, these ASDs have a greater propensity to crystallize when exposed to water than those containing Eudragit L100. The excess solids

recovered at the end of the solubility studies in FaSSIF were also partially crystalline. A more crystalline product was obtained with CIP/HPMCAS-LG, indicating that this ASD is less resistant to crystallization at basic pH. Unlike the ASDs, pure crystalline CIP formed a fully crystalline hydrate in all media; however the PXRD pattern of the residue from solubility studies in water differed from those conducted in FaSSIF and FaSSGF (Figure SI.9d). In the latter two cases, the CIP 3.7 hydrate was indentified,[51] while TGA of the former hydrate found it to contain 14.3% water (Figure SI.10). This corresponds to approximately 3.1 moles of water per mole of CIP. Interestingly, while the HPMCAS-LG ASD also formed the 3.7 hydrate in water, all the other ASD/media combinations resulted in the CIP 3.1 hydrate.

In FaSSIF crystalline CIP reached a peak concentration of 0.9 mg/mL after 1 min. This quickly fell over the first 10 min, and then remained fairly constant at approximately 0.15 mg/mL for the remainder of the study. The sodium taurocholate and lecithin present in FaSSIF mimic bile salts and phospholipids, respectively, in intestinal fluid.[54] The increased solubility of the pure drug in this medium compared to water may be due to the presence of these surfactants. The Eudragit L100 and HPMCAS ASDs behaved differently over the course of the study. The solubility of the former increased gradually over 2 hours, giving the plot in Figure 7b a convex shape. In contrast, the HPMCAS-LG and HPMCAS-MG ASDs reached a peak in CIP concentration after 5–10 min, and then slowly fell over the remainder of the study. The LG grade of HPMCAS reached a top concentration of 1.9 mg/mL, whereas the MG grade obtained a maximum of 1.5 mg/mL. Solid dispersions containing different grades of HPMCAS would be expected to show discrepancies in solubility at various pH values, due to differences in their succinoyl and acetyl content.[55] However, although the former sample remained at a higher concentration for the majority of the study, after 2 hours an equal concentration of 1.3 mg/mL was obtained with both HPMCAS

ASDs. The decrease in the solubility of CIP/HPMCAS-LG over time may be due to the conversion of the drug to its hydrate, as detected by PXRD, as the aqueous solubility and dissolution rate of CIP hydrate is significantly lower than that of the anhydrous drug.[56] Although HPMCAS-LG and HPMCAS-MG are soluble at a pH above 5.5 and 6.0 respectively,[26] this did not result in a substantial increase in the solubility of these ASDs in FaSSIF.

In FaSSGF the Eudragit L100 and HPMCAS-LG ASDs showed very similar behavior to each other, achieving maximum CIP concentrations of 3.2 mg/mL after 2 hours. The HPMCAS-MG formulation was somewhat more soluble at low pH, reaching 4.1 mg/mL (Figure 7c). The solubility of the pure drug however was approximately 3–4 times higher than that of the ASDs. This may be due to the fact that the polymers are insoluble in aqueous acidic solutions.[55] CIP on the other hand has high solubility at pH < 5, as it has a net positive charge. In contrast, it has minimal solubility at neutral pH, where it bears no overall charge.[4] Similar results were seen in solubility studies of malonic, tartaric and oxalic acid salts of CIP, which were also found to be less soluble in acidic media than the pure drug.[10] An amorphous solid was recovered at the end of this study for all of the ASDs, indicating that they are resistant to crystallization at low pH.

The pH of the solutions at the end of the studies was measured and is listed in Figure 7. Very small changes in pH, of ± 0.2 on average, occurred over the course of the study, with the exception of pure CIP in FaSSGF. In this case the high quantity of weakly basic drug in solution increased the pH to 4.7. Therefore, the differences in solubility described above cannot be attributed to changes in pH, but rather to the physical form of the drug and the presence of polymers.

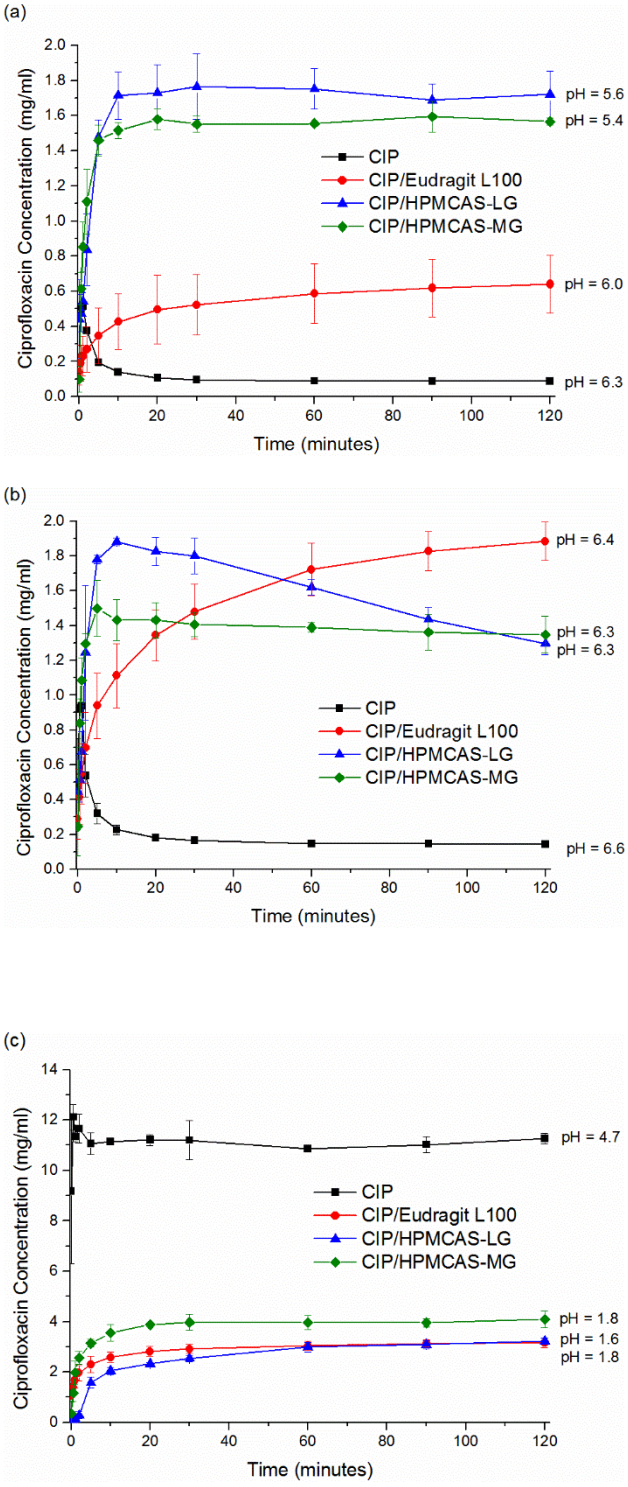

Figure 7. Solubility studies in (a) water (b) FaSSIF and (c) FaSSGF at 37 ºC. The average of at least 3 experiments are plotted, ± the standard deviation. The average pH of the solutions at the end of the study is also shown.

A modification of the Henderson-Hasselbalch equation was used to construct the theoretical pH-solubility profile of pure CIP and the commercial hydrochloride salt, CIP HCl:

$$S_T = [B]\,(1 + 10^{pKa1-pH} + 10^{pH-pKa2}) \quad (4)$$

S_T is the total solubility of the drug in moles/L and [B] is the concentration of the free base (approximately 0.000266 M for CIP and 0.0008 M for CIP HCl). As previously mentioned, the pK_a values of the carboxylic acid (pKa_1) and piperazine amine (pKa_2) of CIP are equal to 6.16, and 8.62, respectively.[38] The CIP ASDs may be considered as basic salts, as they consist of an interaction between the positively charged amino group of the drug and negatively charged carboxylate groups of the polymers. According to Kramer and Flynn, the pH-solubility profile of a basic salt can be represented by two independent solubility profiles, one of which describes when the free base is the saturation species, and the other when the salt is the saturation species.[57] The point at which the two curves intersect is referred to as the pH_{max}, the pH of maximum solubility. In a saturated solution above pH_{max}, the dissolved solute is in equilibrium with the free base, and at a pH below pH_{max}, it is in equilibrium with the salt.[6] The following equation was used to predict the pH-solubility profile of the ASDs:[6]

$$S_T\,(pH<pH_{max}) = [BH^+]_s\,(1 + 10^{pH-pKa}) \quad (5)$$

$[BH^+]_s$ is the concentration of the protonated amorphous salt. The subscript s highlights the fact that the salt is the saturation species at a pH below pH_{max}.[6]

As can be seen from Figure 8, the experimental data does not fit the theoretical pH-solubility curve of CIP exactly. The solubility of the drug from the ASDs in water and FaSSIF is higher than that predicted for CIP. These experimental data points align more closely with the profile of

CIP HCl. Therefore, a more accurate pH_{max} for these salts would be the intersection of the curve for CIP HCl and the CIP ASDs, which occurs at a pH of 5.1. The three main outliers in Figure 8 correspond to the particularly high solubility of the ASDs in FaSSIF. As previously mentioned, FaSSIF contains surfactants, which may enhance the solubility of these solids compared to water. This lack of fit also suggests that the solubility enhancement of these formulations is not due to their effect on pH. Instead this may be attributed to their amorphous nature and polymer content. The solubility of the pure drug in FaSSGF is also higher than that predicted, and aligns more closely with the CIP HCl curve. Due to the presence of HCl in FaSSGF, the drug is likely to be in a similar environment in this medium as CIP HCl in water. At a pH below pH_{max}, i.e. in FaSSGF, the ASDs no longer follow the solubility curve of CIP, as the equilibrium species is now the salt. At acidic pH they may be more accurately described by eq 5 above.

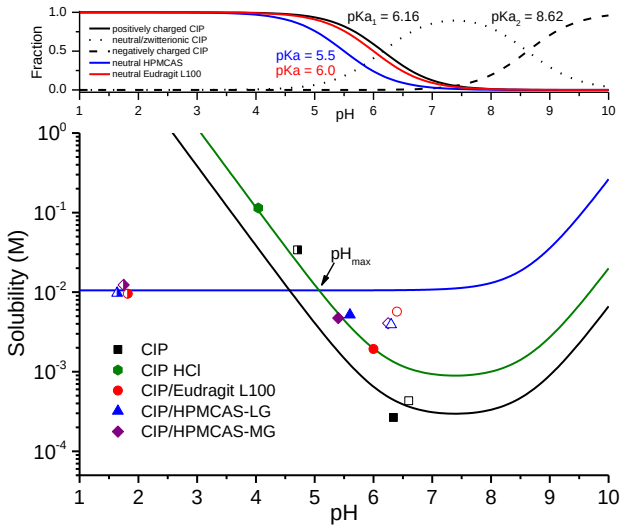

Figure 8. Theoretical pH-solubility profiles of CIP (black), CIP HCl (green), and CIP ASDs (blue). The symbols represent the average concentrations obtained from solubility studies after two hours in water (filled symbols), FaSSIF (empty symbols) and FaSSGF (half-filled symbols).

The plot above shows the distribution of species for CIP, Eudragit L100 and HPMCAS as a function of pH (black lines: CIP; red line: Eudragit L100; and blue line: HPMCAS).

PAMPA Permeability Study

The results of the PAMPA study, under iso-pH and pH gradient conditions, are shown in Table 1. The commercially available hydrochloride salt, CIP HCl, was included in the study for comparison. PAMPA is usually carried out using donor and acceptor solutions of the same pH (iso-pH conditions), however this does not accurately mimic what occurs in vivo. Fortuna et al obtained the best correlation between apparent permeability from PAMPA studies and human intestinal absorption for a range of drugs, including the fluoroquinolone norfloxacin, with a pH of 6.5 and 7.4 in the donor and acceptor compartments, respectively.[58] The pH of the blood and the cytosol of intestinal cells lining the duodenum is about 7.4, therefore this is a suitable pH to use for the acceptor compartment.[59] CIP is believed to be absorbed from the upper section of the duodenum, which has a pH of 6.4.[60,61] A donor/acceptor pH of 6.4/7.4 was therefore chosen for this study in order to more closely represent the pH gradient present in vivo at the site of CIP absorption.[59] In addition, as the permeability of ionizable drugs, such as CIP, depends on pH, it is useful to carry out PAMPA at two different pH values for such compounds, to prevent under- or overestimation of permeability.

Table 1. PAMPA Permeability Values of CIP

	iso-pH		**pH gradient**		
Sample	P_e[a] x 10^6 (cm/s)	log P_e	P_e x 10^6 (cm/s)	log P_e	*p*-value[b]

Crystalline CIP	0.56 ± 0.06	-6.25 ± 0.05	0.62 ± 0.08	-6.21 ± 0.05	0.42
CIP HCl	0.32 ± 0.00	-6.50 ± 0.01	0.32 ± 0.01	-6.49 ± 0.01	0.22
CIP/Eudragit L100	0.52 ± 0.00	-6.28 ± 0.00	0.50 ± 0.06	-6.31 ± 0.05	0.50
CIP/HPMCAS -LG	0.75 ± 0.06	-6.13 ± 0.04	0.64 ± 0.10	-6.20 ± 0.07	0.20
CIP/HPMCAS -MG	0.64 ± 0.03	-6.19 ± 0.02	0.67 ± 0.03	-6.18 ± 0.02	0.34

[a] P_e: effective permeability. The average of three measurements is shown, ± the standard deviation.

[b] *p*-value from *t* test comparing P_e from regular and pH-gradient PAMPA.

According to Sugano, a permeability of less than 1×10^{-6} cm/s (or log $P_e < -6$) can be considered as low permeability.[62] As can be seen from Table 1, all of the samples are poorly permeable, with a $P_e < 1 \times 10^{-6}$ cm/s. A similarly low P_e of 0.19×10^{-6} cm/s for CIP was obtained by Tehler et al in Caco-2 studies.[63] Two-sample *t* tests were used to compare the results of the individual samples under both pH conditions, and in each case no statistically significant difference was found (see *p*-values in Table 1). The pI of CIP is around 7.4–7.5.[64] The passive absorption of this drug would therefore be expected to be highest at this pH. As the pH is decreased below the pI, the carboxylate group of CIP will become protonated, and the proportion of drug bearing an overall positive charge will increase. This should reduce its passive transport through a lipid membrane. However, at neutral pH the drug exists primarily as the zwitterion, with only about 2% expected to be present in the unionized form at the pI.[64] While the membrane penetration and diffusion of unionized CIP is energetically favorable, the transmembrane translocation of zwitterionic CIP is unlikely to occur.[65] Evidently, dropping from pH 7.4 to 6.4 does not have a large effect on the proportion of

unionized CIP present, and thus no significant difference in P_e was seen when the donor solution pH was changed in the above study.

ANOVA and Tukey's multiple comparison test were carried out to compare the P_e of the different samples. CIP from ASDs containing HPMCAS-LG and HPMCAS-MG possessed the highest permeability, with a P_e of 0.75×10^{-6} and 0.64×10^{-6} cm/s, respectively under iso-pH conditions, and 0.64×10^{-6} and 0.67×10^{-6} cm/s, respectively, with a pH-gradient; however these samples were not statistically significantly different from each other under either pH condition. In addition, the CIP/HPMCAS-MG system did not differ significantly from the pure drug in either study, while CIP from the HPMCAS-LG sample was only significantly more permeable than CIP under iso-pH conditions. CIP as the HCl salt on the other hand had a significantly lower permeability than the other samples, with a P_e of 0.32×10^{-6} cm/s under both pH conditions. The drug from the ASD containing Eudragit L100 had a slightly lower average P_e than the pure crystalline drug in both PAMPA experiments; however this difference was not statistically significant. The lower P_e obtained with the CIP/Eudragit L100 ASD compared to those containing HPMCAS may be due to the formation of drug/polymer complexes in solution. As shown previously by Friesen et al, upon addition to aqueous solutions, ASDs may rapidly disperse to form a number of species.[66] These can potentially include large drug/polymer aggregates, which may form a slowly dissolving amorphous precipitate, and thus reduce the concentration of free drug in solution.[66] This would be more likely to occur with CIP/Eudragit L100 due to the stronger drug-polymer interactions present in this ASD, as suggested by its particularly high T_g.

A number of studies have found that other solubility enhancing formulations such as cyclodextrins, surfactants and cosolvents decrease the permeability of drugs in both PAMPA and

intestinal perfusion assays, leading to a trade-off between solubility and permeability.[21,67] According to Miller et al, preparations such as these increase the equilibrium solubility of drugs, which results in a decrease in their apparent cell membrane/intestinal lumen partition coefficient. As the permeability of a drug is directly related to this coefficient, the solubility advantage provided by these formulations is accompanied by a decrease in permeability.[67] In contrast, ASDs increase the solubility of drugs via supersaturation, which does not affect the apparent membrane/lumen partition coefficient. Amorphous formulations can therefore significantly increase the concentration of drug in solution, while also maintaining a constant effective permeability, giving them a superior solubility-permeability balance.[21,67] The results of this study are therefore in line with those of other researchers, with all of the CIP ASDs enhancing the solubility of the drug in water and FaSSIF, without a subsequent decrease in permeability. The crystalline CIP HCl salt on the other hand significantly reduced the permeability of the drug, most likely due to greater ionization of CIP. Although the P_e of a drug is not affected by its concentration (as long as the drug is free to pass through the membrane), the increased solubility afforded by ASDs should increase the transmembrane flux of a drug, and thus may also improve its in vivo absorption.[67]

According to Tam et al, 18% of CIP is absorbed via the paracellular route at pH 6.5.[68] As the PAMPA model does not take account of paracellular transport, it is possible that the results above underestimate the in vivo absorption of CIP. PAMPA is also unable to predict active transport, and will therefore underestimate the permeability of compounds which are absorbed via drug transporters.[69] This could explain why the effective permeability of CIP reported here is lower than that obtained by others in rat in situ and Caco-2 cell studies.[68,70] While CIP is mainly absorbed by passive transport, it is also a substrate for active transporters in the intestine, such as

organic anion transporting polypeptide 1A2 (OATP1A2).[71] In addition, it is a substrate for the efflux protein breast cancer resistance protein (BCRP), which reduces the bioavailability of the drug.[72] Despite this, Bermejo et al showed that for fluoroquinolones such as CIP, there was a good correlation between the results of PAMPA and that of Caco-2 and rat in situ permeability studies.[38] As the main aim of the permeability assay performed in this study was to determine whether ASD formation affects the permeability of CIP, PAMPA was suitable for this comparative analysis. However, in order to obtain a more accurate quantitative estimate of the permeability of the drug and ASDs, more representative permeability studies would be required, such as rat in situ perfusion assays, which more closely mimic the environment *in vivo*.

Bacterial Studies

The minimum inhibitory concentration (MIC) and minimum bactericidal concentration (MBC) of CIP and the ASDs in a number of bacterial species are shown in Table 2. The values that differ significantly from those of pure crystalline CIP are shown in bold. The MBC is expected to be larger than the MIC, as a larger quantity of API is required to kill bacteria rather than just inhibit their growth. MICs ≤ 1.0 μg/mL indicate that the microorganism is susceptible to CIP, whereas MICs ≥ 2.0 μg/mL indicate resistance to this antibiotic.[73] All of the organisms used in this study can therefore be considered as sensitive to CIP, with MICs ≤ 1 μg/mL. The MIC and MBC values obtained with CIP are close to those obtained by other researchers in these species.[74–76] *E. coli* was found to be the most susceptible strain to CIP, with a MIC of 0.008–0.032 μg/mL. This was followed by *K. pneumoniae* (MIC 0.032–0.125 μg/mL), *P. aeruginosa* (MIC 0.125–1.0 μg/mL) and *S. aureus* (MIC 0.25–1.0 μg/mL). The MBCs also followed the same order of susceptibility. A drug is generally considered bactericidal if it has a MBC to MIC ratio of ≤ 4.[77] Therefore, all of the samples in this study were bactericidal, with ratios of 1–2.

The formulation of CIP as an ASD did not result in a decrease in antibacterial activity in any case. In fact, CIP/ HPMCAS-MG had a significantly lower MIC and MBC in all bacterial species studied compared to the pure drug. The MIC of HPMCAS-LG was also significantly improved in *E. coli*, while its MBC decreased in both *E. coli* and *S. aureus*. As described above, these ASDs had the highest P_e in PAMPA permeability studies, whereas CIP/Eudragit L100 did not differ significantly from the pure drug. Therefore, the improved permeability of these samples may have aided the penetration of CIP into the bacterial cells, most likely via the passive diffusion route through the cell membranes.

Table 2. Minimum Inhibitory Concentration and Minimum Bactericidal Concentration of Ciprofloxacin and ASDs in Various Bacteria

Sample	***S. aureus***	***E. coli***	***P. aeruginosa***	***K. pneumoniae***
Minimum Inhibitory Concentration (μg/mL)				
CIP	1	0.032	0.5	0.125
CIP/Eudragit L100	1	0.032	0.5–1	0.125
CIP/HPMCAS-LG	0.5	**0.008–0.016**	0.25–0.5	0.063–0.125
CIP/HPMCAS-MG	**0.25–0.5**	**0.008–0.016**	**0.125–0.25**	**0.032–0.063**
Minimum Bactericidal Concentration (μg/mL)				
CIP	1.0–2.0	0.032–0.064	1.0	0.25
CIP/Eudragit L100	1	0.032	1.0	0.25
CIP/HPMCAS-LG	**0.5**	**0.016**	1.0	0.125
CIP/HPMCAS-MG	**0.5**	**0.016**	**0.25–0.5**	**0.063–0.125**

Conclusions

Amorphous solid dispersions are one formulation option for poorly soluble drugs, however the polymers used in these preparations must be carefully chosen. This work has shown that an acidic polymer is necessary to produce CIP ASDs by ball milling, as it enables the formation of stabilizing ionic interactions between the two components. These bonds resulted in high T_g values, above those predicted by the Gordon-Taylor equation. While the CIP ASDs crystallized quickly under accelerated stability conditions of 40 ºC/75% RH, they remained amorphous following exposure to humidity levels of up to 90% at 25 ºC during DVS analysis. Therefore, although the stabilizing effects of the polymers were not sufficient to prevent crystallization of CIP when exposed to a combination of high heat and humidity, these ASDs could be expected to remain stable if stored at ambient temperatures.

The ASDs chosen for further examination showed superior solubility in water and FaSSIF compared to the pure drug, which can be attributed to their amorphous nature, rather than any effect on pH. The polymer content of the ASDs also enabled the maintenance of supersaturation for at least two hours in most cases. In addition, no decrease in the passive permeability of CIP occurred with any of these ASDs, while a modest increase in effective permeability was seen with the ASD containing HPMCAS-LG. In contrast, the crystalline CIP HCl salt significantly decreased the permeability of the drug, highlighting the benefit of amorphous polymeric formulations in this regard. In line with the results of the permeability assay, the formulation of CIP as an ASD did not reduce its antibacterial potency in the bacterial species studied, and a decrease in MIC and MBC was also obtained with the ASDs containing HPMCAS. This indicates that ASD formation with HPMCAS increases the proportion of CIP capable of diffusing through bacterial cell membranes. Therefore, ASDs may be a viable alternative for formulating CIP with improved solubility, bioavailability and antibacterial activity.

Associated Content

Supporting Information.

PXRD and FTIR analysis of semi-crystalline solid dispersions; TGA of CIP and ASDs; chemical structure of polymers; PXRD analysis following DVS and solubility studies; and TGA of CIP hydrate. This material is available free of charge via the Internet at http://pubs.acs.org.

Author Information

Corresponding Author

*Phone: +35318962787, email: ltajber@tcd.ie.

Funding Sources

Funding for this research was provided by the Science Foundation Ireland under Grant No. 12/RC/2275 (Synthesis and Solid State Pharmaceutical Centre).

Notes

The authors declare no competing financial interest.

References

(1) Mesallati, H.; Mugheirbi, N. A.; Tajber, L. Two Faces of Ciprofloxacin: Investigation of Proton Transfer in Solid State Transformations. *Cryst. Growth Des.* **2016**, *16*, 6574–85.

(2) Paluch, K. J.; McCabe, T.; Müller-Bunz, H.; Corrigan, O. I.; Healy, A. M.; Tajber, L. Formation and Physicochemical Properties of Crystalline and Amorphous Salts with Different Stoichiometries Formed between Ciprofloxacin and Succinic Acid. *Mol. Pharm.* **2013**, *10*, 3640–3654.

(3) Zhang, C.-L.; Zhao, F.; Wang, Y. Thermodynamics of the Solubility of Ciprofloxacin in Methanol, Ethanol, 1-Propanol, Acetone, and Chloroform from 293.15 to 333.15K. *J. Mol. Liq.* **2010**, *156*, 191–193.

(4) Breda, S. A.; Jimenez-Kairuz, A. F.; Manzo, R. H.; Olivera, M. E. Solubility Behavior and Biopharmaceutical Classification of Novel High-Solubility Ciprofloxacin and Norfloxacin Pharmaceutical Derivatives. *Int. J. Pharm.* **2009**, *371*, 106–113.

(5) Zaki, N. M.; Artursson, P.; Bergström, C. A. S. A Modified Physiological BCS for Prediction of Intestinal Absorption in Drug Discovery. *Mol. Pharm.* **2010**, *7*, 1478–1487.

(6) Serajuddin, A. T. M. Salt Formation to Improve Drug Solubility. *Adv. Drug Deliv. Rev.* **2007**, *59*, 603–616.

(7) Parojčić, J.; Stojković, A.; Tajber, L.; Grbić, S.; Paluch, K. J.; Djurić, Z.; Corrigan, O. I. Biopharmaceutical Characterization of Ciprofloxacin HCl-Ferrous Sulfate Interaction. *J. Pharm. Sci.* **2011**, *100*, 5174–5184.

(8) Florence, A. T.; Attwood, D. *Physicochemical Principles of Pharmacy*; 5th ed.; Pharmaceutical Press: Cornwall, 2011.

(9) Yeon, K. .; Kim, J. H.; Choi, K. E.; Kim, D. H.; Lee, K. H. Salts of a Quinolone-Carboxylic Acid. U.S. Patent US5484785 A, 1996.

(10) Reddy, J. S.; Ganesh, S. V.; Nagalapalli, R.; Dandela, R.; Solomon, K. A.; Kumar, K. A.; Goud, N. R.; Nangia, A. Fluoroquinolone Salts with Carboxylic Acids. *J. Pharm. Sci.* **2011**, *100*, 3160–3176.

(11) Florindo, C.; Costa, A.; Matos, C.; Nunes, S. L.; Matias, A. N.; Duarte, C. M. M.; Rebelo, L. P. N.; Branco, L. C.; Marrucho, I. M. Novel Organic Salts Based on Fluoroquinolone Drugs: Synthesis, Bioavailability and Toxicological Profiles. *Int. J. Pharm.* **2014**, *469*, 179–189.

(12) Romañuk, C. B.; Manzo, R. H.; Linck, Y. G.; Chattah, A. K.; Monti, G. A.; Olivera, M. E. Characterization of the Solubility and Solid-State Properties of Saccharin Salts of Fluoroquinolones. *J. Pharm. Sci.* **2009**, *98*, 3788–3801.

(13) Willis, C. R.; Banker, G. S. Polymer–drug Interacted Systems in the Physicochemical Design of Pharmaceutical Dosage Forms I. Drug Salts with PVM/MA and with a PVM/MA Hemi-Ester. *J. Pharm. Sci.* **1968**, *57*, 1598–1603.

(14) Yu, L. Amorphous Pharmaceutical Solids: Preparation, Characterization and Stabilization. *Adv. Drug Deliv. Rev.* **2001**, *48*, 27–42.

(15) Al-Obaidi, H.; Buckton, G. Evaluation of Griseofulvin Binary and Ternary Solid Dispersions with HPMCAS. *AAPS PharmSciTech* **2009**, *10*, 1172–1177.

(16) Huang, Y.; Dai, W.-G. Fundamental Aspects of Solid Dispersion Technology for Poorly Soluble Drugs. *Acta Pharm. Sin. B* **2014**, *4*, 18–25.

(17) Shamblin, S. L.; Zografi, G. The Effects of Absorbed Water on the Properties of Amorphous Mixtures Containing Sucrose. *Pharm. Res.* **1999**, *16*, 1119–1124.

(18) Guzmán, H. R.; Tawa, M.; Zhang, Z.; Ratanabanangkoon, P.; Shaw, P.; Gardner, C. R.; Chen, H.; Moreau, J.-P.; Almarsson, O.; Remenar, J. F. Combined Use of Crystalline Salt Forms and Precipitation Inhibitors to Improve Oral Absorption of Celecoxib from Solid Oral Formulations. *J. Pharm. Sci.* **2007**, *96*, 2686–2702.

(19) Cheow, W. S.; Hadinoto, K. Self-Assembled Amorphous Drug-Polyelectrolyte Nanoparticle Complex with Enhanced Dissolution Rate and Saturation Solubility. *J. Colloid Interface Sci.* **2012**, *367*, 518–526.

(20) Osman, R.; Kan, P. L.; Awad, G.; Mortada, N.; El-Shamy, A.-E.; Alpar, O. Spray Dried Inhalable Ciprofloxacin Powder with Improved Aerosolisation and Antimicrobial Activity. *Int. J. Pharm.* **2013**, *449*, 44–58.

(21) Beig, A.; Miller, J. M.; Lindley, D.; Carr, R. A.; Zocharski, P.; Agbaria, R.; Dahan, A. Head-to-Head Comparison of Different Solubility-Enabling Formulations of Etoposide and Their Consequent Solubility-Permeability Interplay. *J. Pharm. Sci.* **2015**, *104*, 2941–2947.

(22) Gordon, M.; Taylor, J. S. Ideal Copolymers and the Second-Order Transitions of Synthetic Rubbers. I. Non-Crystalline Copolymers. *J. Appl. Chem.* **1952**, *2*, 493–500.

(23) Lu, Q.; Zografi, G. Phase Behavior of Binary and Ternary Amorphous Mixtures Containing Indomethacin, Citric Acid, and PVP. *Pharm. Res.* **1998**, *15*, 1202–1206.

(24) Evonik Industries. EUDRAGIT® L 100 http://eudragit.evonik.com/product/eudragit/en/products-services/eudragit-products/enteric-formulations/l-100/Pages/default.aspx (accessed Feb 18, 2015).

(25) Evonik Industries. EUDRAGIT® L 100-55

http://eudragit.evonik.com/product/eudragit/en/products-services/eudragit-products/enteric-formulations/l-100-55/pages/default.aspx.

(26) Ashland. AquaSolve hydroxypropylmethylcellulose acetate succinate http://www.ashland.com/Ashland/Static/Documents/ASI/PC_12624_AquaSolve_AS_Handbook.pdf (accessed Feb 11, 2015).

(27) Evonik Industries. EUDRAGIT® L 100 and EUDRAGIT® S 100 http://eudragit.evonik.com/sites/lists/HN/ProductSpecifications/TI-EUDRAGIT-L-100-S-100-EN.pdf (accessed Jan 11, 2016).

(28) Evonik Industries. EUDRAGIT® L 100-55 http://eudragit.evonik.com/sites/lists/HN/ProductSpecifications/TI-EUDRAGIT-L-100-55-EN.pdf (accessed Jan 11, 2016).

(29) Xiang, T.-X.; Anderson, B. D. Molecular Dynamics Simulation of Amorphous Hydroxypropyl-Methylcellulose Acetate Succinate (HPMCAS): Polymer Model Development, Water Distribution, and Plasticization. *Mol. Pharm.* **2014**, *11*, 2400–2411.

(30) Merck Millipore. *Lipid-PAMPA with the MultiScreen® Filter Plates*; Billerica, MA, 2004.

(31) Wohnsland, F.; Faller, B. High-Throughput Permeability pH Profile and High-Throughput Alkane/water Log P with Artificial Membranes. *J. Med. Chem.* **2001**, *44*, 923–930.

(32) Schmidt, D.; Lynch, J. *MultiScreen Filter Plates for PAMPA - Evaluation of the Reproducibility of Parallel Artificial Membrane Permeation Assays (PAMPA)*; Massachusetts, 2003.

(33) Umerska, A.; Cassisa, V.; Matougui, N.; Joly-Guillou, M.-L.; Eveillard, M.; Saulnier, P.

Antibacterial Action of Lipid Nanocapsules Containing Fatty Acids or Monoglycerides as Co-Surfactants. *Eur. J. Pharm. Biopharm.* **2016**, *108*, 100–110.

(34) Descamps, M.; Willart, J. F.; Dudognon, E.; Caron, V. Transformation of Pharmaceutical Compounds upon Milling and Comilling: The Role of T(g). *J. Pharm. Sci.* **2007**, *96*, 1398–1407.

(35) Yang, Z.; Nollenberger, K.; Albers, J.; Qi, S. Molecular Implications of Drug-Polymer Solubility in Understanding the Destabilization of Solid Dispersions by Milling. *Mol. Pharm.* **2014**, *11*, 2453–2465.

(36) Yang, J.; Grey, K.; Doney, J. An Improved Kinetics Approach to Describe the Physical Stability of Amorphous Solid Dispersions. *Int. J. Pharm.* **2010**, *384*, 24–31.

(37) Dorofeev, V. L. The Betainelike Structure and Infrared Spectra of Drugs of the Fluoroquinolone Group. *Pharm. Chem. J.* **2004**, *38*, 698–702.

(38) Bermejo, M.; Avdeef, A.; Ruiz, A.; Nalda, R.; Ruell, J. A.; Tsinman, O.; González, I.; Fernández, C.; Sánchez, G.; Garrigues, T. M.; et al. PAMPA--a Drug Absorption in Vitro Model 7. Comparing Rat in Situ, Caco-2, and PAMPA Permeability of Fluoroquinolones. *Eur. J. Pharm. Sci.* **2004**, *21*, 429–441.

(39) Lubrizol. *Pharmaceutical Bulletin 23: Bioadhesion*; Wickliffe, Ohio, 2011.

(40) Huang, K.-S.; Britton, D.; Margaret, L.; C. Etter, T.; Byrn, S. R. A Novel Class of Phenol–pyridine Co-Crystals for Second Harmonic Generation. *J. Mater. Chem.* **1997**, *7*, 713–720.

(41) Weuts, I.; Kempen, D.; Verreck, G.; Peeters, J.; Brewster, M.; Blaton, N.; Van den Mooter, G. Salt Formation in Solid Dispersions Consisting of Polyacrylic Acid as a Carrier and

Three Basic Model Compounds Resulting in Very High Glass Transition Temperatures and Constant Dissolution Properties upon Storage. *Eur. J. Pharm. Sci.* **2005**, *25*, 387–393.

(42) Song, Y.; Yang, X.; Chen, X.; Nie, H.; Byrn, S.; Lubach, J. W. Investigation of Drug–Excipient Interactions in Lapatinib Amorphous Solid Dispersions Using Solid-State NMR Spectroscopy. *Mol. Pharm.* **2015**, *12*, 857–866.

(43) Maniruzzaman, M.; Morgan, D. J.; Mendham, A. P.; Pang, J.; Snowden, M. J.; Douroumis, D. Drug-Polymer Intermolecular Interactions in Hot-Melt Extruded Solid Dispersions. *Int. J. Pharm.* **2013**, *443*, 199–208.

(44) Borbas, E.; Sinko, B.; Tsinman, O.; Tsinman, K.; Kiserdei, E.; Demuth, B.; Balogh, A.; Bodak, B.; Domokos, A.; Dargo, G.; et al. Investigation and Mathematical Description of the Real Driving Force of Passive Transport of Drug Molecules from Supersaturated Solutions. *Mol. Pharm.* **2016**, *13*, 3816–26.

(45) Brostow, W.; Chiu, R.; Kalogeras, I. M.; Vassilikou-Dova, A. Prediction of Glass Transition Temperatures: Binary Blends and Copolymers. *Mater. Lett.* **2008**, *62*, 3152–3155.

(46) Jensen, K. T.; Löbmann, K.; Rades, T.; Grohganz, H. Improving Co-Amorphous Drug Formulations by the Addition of the Highly Water Soluble Amino Acid, Proline. *Pharmaceutics* **2014**, *6*, 416–435.

(47) Tong, P.; Taylor, L. S.; Zografi, G. Influence of Alkali Metal Counterions on the Glass Transition Temperature of Amorphous Indomethacin Salts. *Pharm. Res.* **2002**, *19*, 649–654.

(48) van Drooge, D. J.; Hinrichs, W. L. J.; Visser, M. R.; Frijlink, H. W. Characterization of the Molecular Distribution of Drugs in Glassy Solid Dispersions at the Nano-Meter Scale,

Using Differential Scanning Calorimetry and Gravimetric Water Vapour Sorption Techniques. *Int. J. Pharm.* **2006**, *310*, 220–229.

(49) Konno, H.; Taylor, L. S. Influence of Different Polymers on the Crystallization Tendency of Molecularly Dispersed Amorphous Felodipine. *J. Pharm. Sci.* **2006**, *95*, 2692–2705.

(50) Andronis, V.; Yoshioka, M.; Zografi, G. Effects of Sorbed Water on the Crystallization of Indomethacin from the Amorphous State. *J. Pharm. Sci.* **1997**, *86*, 346–351.

(51) Mafra, L.; Santos, S. M.; Siegel, R.; Alves, I.; Paz, F. A. A.; Dudenko, D.; Spiess, H. W. Packing Interactions in Hydrated and Anhydrous Forms of the Antibiotic Ciprofloxacin: A Solid-State NMR, X-Ray Diffraction, and Computer Simulation Study. *J. Am. Chem. Soc.* **2012**, *134*, 71–4.

(52) Chawla, G.; Bansal, A. K. A Comparative Assessment of Solubility Advantage from Glassy and Crystalline Forms of a Water-Insoluble Drug. *Eur. J. Pharm. Sci.* **2007**, *32*, 45–57.

(53) Warren, D. B.; Benameur, H.; Porter, C. J. H.; Pouton, C. W. Using Polymeric Precipitation Inhibitors to Improve the Absorption of Poorly Water-Soluble Drugs: A Mechanistic Basis for Utility. *J. Drug Target.* **2010**, *18*, 704–731.

(54) biorelevant.com. FaSSIF, FeSSIF & FaSSGF contain bile salts and phospholipids http://biorelevant.com/fassif-fessif-fassgf-powder/contains-bile-salts-phospholipids/ (accessed Feb 18, 2015).

(55) Tanno, F.; Nishiyama, Y.; Kokubo, H.; Obara, S. Evaluation of Hypromellose Acetate Succinate (HPMCAS) as a Carrier in Solid Dispersions. *Drug Dev. Ind. Pharm.* **2004**, *30*, 9–17.

(56) Li, X.; Zhi, F.; Hu, Y. Investigation of Excipient and Processing on Solid Phase Transformation and Dissolution of Ciprofloxacin. *Int. J. Pharm.* **2007**, *328*, 177–182.

(57) Kramer, S. F.; Flynn, G. L. Solubility of Organic Hydrochlorides. *J. Pharm. Sci.* **1972**, *61*, 1896–1904.

(58) Fortuna, A.; Alves, G.; Soares-da-Silva, P.; Falcão, A. Optimization of a Parallel Artificial Membrane Permeability Assay for the Fast and Simultaneous Prediction of Human Intestinal Absorption and Plasma Protein Binding of Drug Candidates: Application to Dibenz[b,f]azepine-5-Carboxamide Derivatives. *J. Pharm. Sci.* **2012**, *101*, 530–540.

(59) Avdeef, A. *Absorption and Drug Development: Solubility, Permeability, and Charge State*; John Wiley & Sons, Inc.: New Jersey, 2003.

(60) Harder, S.; Fuhr, U.; Beermann, D.; Staib, A. H. Ciprofloxacin Absorption in Different Regions of the Human Gastrointestinal Tract. Investigations with the Hf-Capsule. *Br. J. Clin. Pharmacol.* **1990**, *30*, 35–39.

(61) Said, H. M.; Blair, J. A.; Lucas, M. L.; Hilburn, M. E. Intestinal Surface Acid Microclimate in Vitro and in Vivo in the Rat. *J. Lab. Clin. Med.* **1986**, *107*, 420–424.

(62) Sugano, K. Permeability of a Drug. In *Biopharmaceutics modeling and simulations: theory, practice, methods, and applications*; John Wiley & Sons: New Jersey, 2012; p. 170.

(63) Tehler, U.; Fagerberg, J. H.; Svensson, R.; Larhed, M.; Artursson, P.; Bergström, C. A. S. Optimizing Solubility and Permeability of a Biopharmaceutics Classification System (BCS) Class 4 Antibiotic Drug Using Lipophilic Fragments Disturbing the Crystal Lattice. *J. Med. Chem.* **2013**, *56*, 2690–2694.

(64) Sun, J.; Sakai, S.; Tauchi, Y.; Deguchi, Y.; Chen, J.; Zhang, R.; Morimoto, K. Determination of Lipophilicity of Two Quinolone Antibacterials, Ciprofloxacin and Grepafloxacin, in the Protonation Equilibrium. *Eur. J. Pharm. Biopharm.* **2002**, *54*, 51–58.

(65) Cramariuc, O.; Rog, T.; Javanainen, M.; Monticelli, L.; Polishchuk, A. V; Vattulainen, I. Mechanism for Translocation of Fluoroquinolones across Lipid Membranes. *Biochim. Biophys. Acta* **2012**, *1818*, 2563–2571.

(66) Friesen, D. T.; Shanker, R.; Crew, M.; Smithey, D. T.; Curatolo, W. J.; Nightingale, J. A. S. Hydroxypropyl Methylcellulose Acetate Succinate-Based Spray-Dried Dispersions: An Overview. *Mol. Pharm.* **2008**, *5*, 1003–1019.

(67) Miller, J. M.; Beig, A.; Carr, R. A.; Spence, J. K.; Dahan, A. A Win-Win Solution in Oral Delivery of Lipophilic Drugs: Supersaturation via Amorphous Solid Dispersions Increases Apparent Solubility without Sacrifice of Intestinal Membrane Permeability. *Mol. Pharm.* **2012**, *9*, 2009–2016.

(68) Tam, K. Y.; Avdeef, A.; Tsinman, O.; Sun, N. The Permeation of Amphoteric Drugs through Artificial Membranes--an in Combo Absorption Model Based on Paracellular and Transmembrane Permeability. *J. Med. Chem.* **2010**, *53*, 392–401.

(69) Markovic, B. D.; Vladimirov, S. M.; Cudina, O. A.; Odovic, J. V; Karljikovic-Rajic, K. D. A PAMPA Assay as Fast Predictive Model of Passive Human Skin Permeability of New Synthesized Corticosteroid C-21 Esters. *Molecules* **2012**, *17*, 480–491.

(70) Rodríguez-Ibáñez, M.; Sánchez-Castaño, G.; Montalar-Montero, M.; Garrigues, T. M.; Bermejo, M.; Merino, V. Mathematical Modelling of in Situ and in Vitro Efflux of

Ciprofloxacin and Grepafloxacin. *Int. J. Pharm.* **2006**, *307*, 33–41.

(71) Maeda, T.; Takahashi, K.; Ohtsu, N.; Oguma, T.; Ohnishi, T.; Atsumi, R.; Tamai, I. Identification of Influx Transporter for the Quinolone Antibacterial Agent Levofloxacin. *Mol. Pharm.* **2007**, *4*, 85–94.

(72) Merino, G.; Alvarez, A. I.; Pulido, M. M.; Molina, A. J.; Schinkel, A. H.; Prieto, J. G. Breast Cancer Resistance Protein (BCRP/ABCG2) Transports Fluoroquinolone Antibiotics and Affects Their Oral Availability, Pharmacokinetics, and Milk Secretion. *Drug Metab. Dispos.* **2006**, *34*, 690–695.

(73) Barry, A. L.; Fass, R. J.; Anhalt, J. P.; Neu, H. C.; Thornsberry, C.; Tilton, R. C.; Painter, B. G.; Washington, J. A. 2nd. Ciprofloxacin Disk Susceptibility Tests: Interpretive Zone Size Standards for 5-Microgram Disks. *J. Clin. Microbiol.* **1985**, *21*, 880–883.

(74) Barry, A. L.; Jones, R. N.; Thornsberry, C.; Ayers, L. W.; Gerlach, E. H.; Sommers6, A. H. M. Antibacterial Activities of Ciprofloxacin, Norfloxacin, Oxolinic Acid, Cinoxacin, and Nalidixic Acid. *Antimicrob. Agents Chemother.* **1984**, *25*, 633–637.

(75) Standiford, H. C.; Drusano, G. L.; Forrest, A.; Tatem, B.; Plaisance3, K. Bactericidal Activity of Ciprofloxacin Compared with that of Cefotaxime in Normal Volunteers. *Antimicrob. Agents Chemother.* **1987**, *31*, 1177–1182.

(76) Well, M.; Naber, K. G.; Kinzig-Schippers, M.; Sörgel, F. Urinary Bactericidal Activity and Pharmacokinetics of Enoxacin versus Norfloxacin and Ciprofloxacin in Healthy Volunteers after a Single Oral Dose. *Int. J. Antimicrob. Agents* **1998**, *10*, 31–38.

(77) Pankey, G. A.; Sabath, L. D. Clinical Relevance of Bacteriostatic versus Bactericidal

Mechanisms of Action in the Treatment of Gram-Positive Bacterial Infections. *Clin. Infect. Dis.* **2004**, *38*, 864–870.

Supporting Information

Amorphous polymeric drug salts as ionic solid dispersion forms of ciprofloxacin

Hanah Mesallati[†], Anita Umerska[$], Krzysztof J. Paluch[§] and Lidia Tajber*[,†]

[†]Synthesis and Solid State Pharmaceutical Centre, School of Pharmacy and Pharmaceutical Sciences, Trinity College Dublin, College Green, Dublin 2, Ireland.

[$]MINT, UNIV Angers, INSERM 1066, CNRS 6021, Universite Bretagne Loire, 4 rue Larrey, Angers 49933 Cedex, France

[§]School of Pharmacy and Medical Sciences, Faculty of Life Sciences, University of Bradford, Bradford, West Yorkshire, BD7 1DP, United Kingdom.

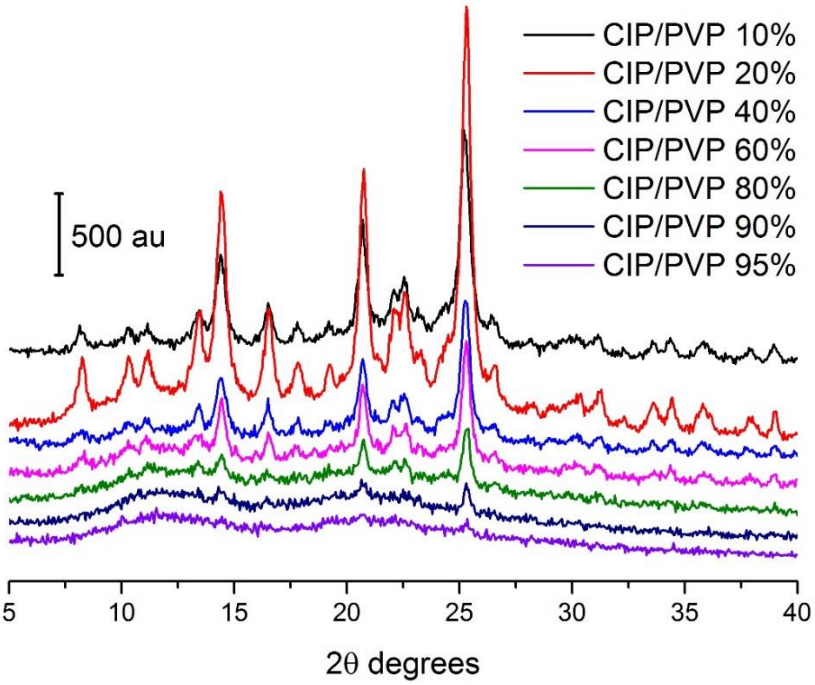

Figure SI.1. PXRD analysis of partially crystalline CIP solid dispersions containing various (w/w) concentrations of PVP.

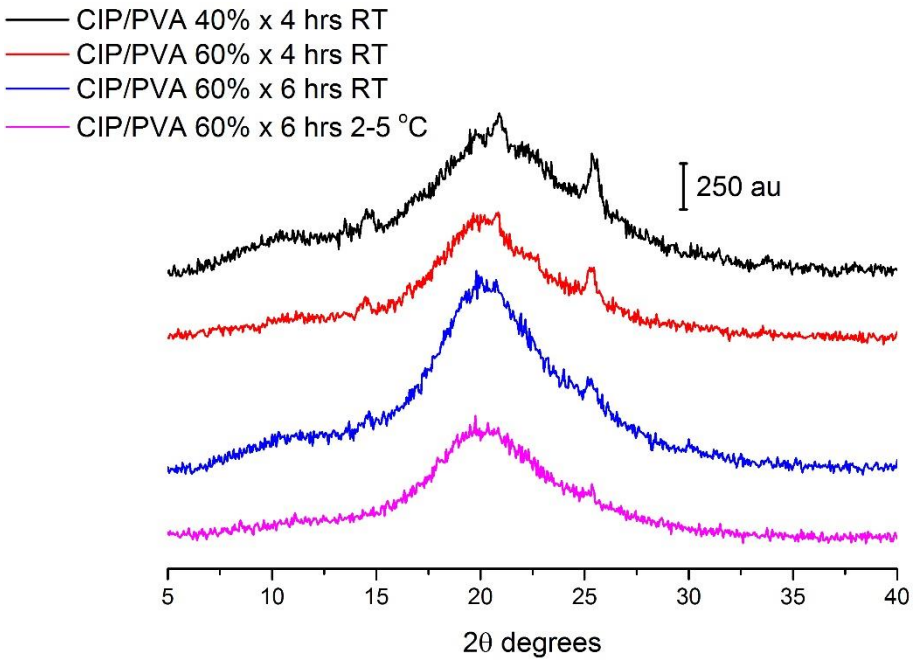

Figure SI.2. PXRD analysis of partially crystalline solid dispersions formed by milling CIP with 40–60% (w/w) PVA at room temperature (RT) or 2–5 °C.

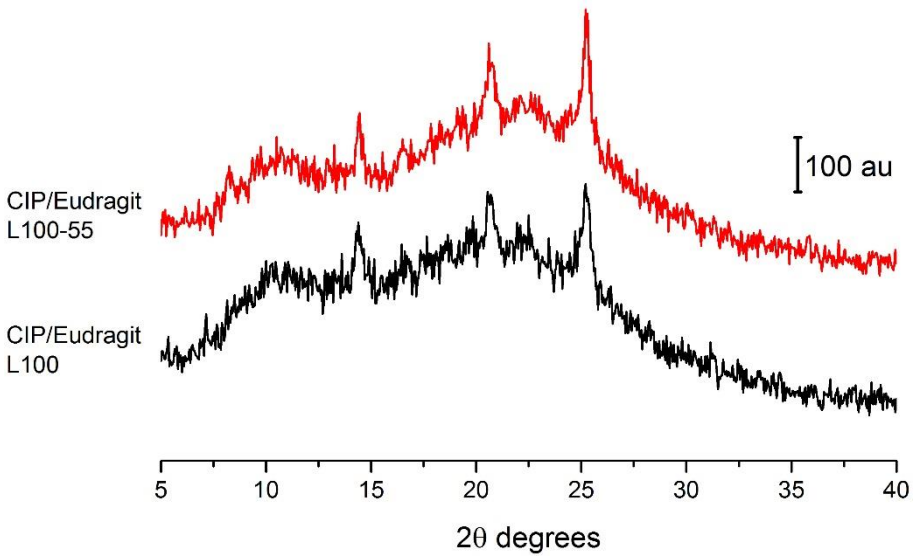

Figure SI.3. PXRD analysis of partially crystalline solid dispersions formed by milling CIP with 20% (w/w) Eudragit L100 and Eudragit L100-55 for 4 hours at room temperature.

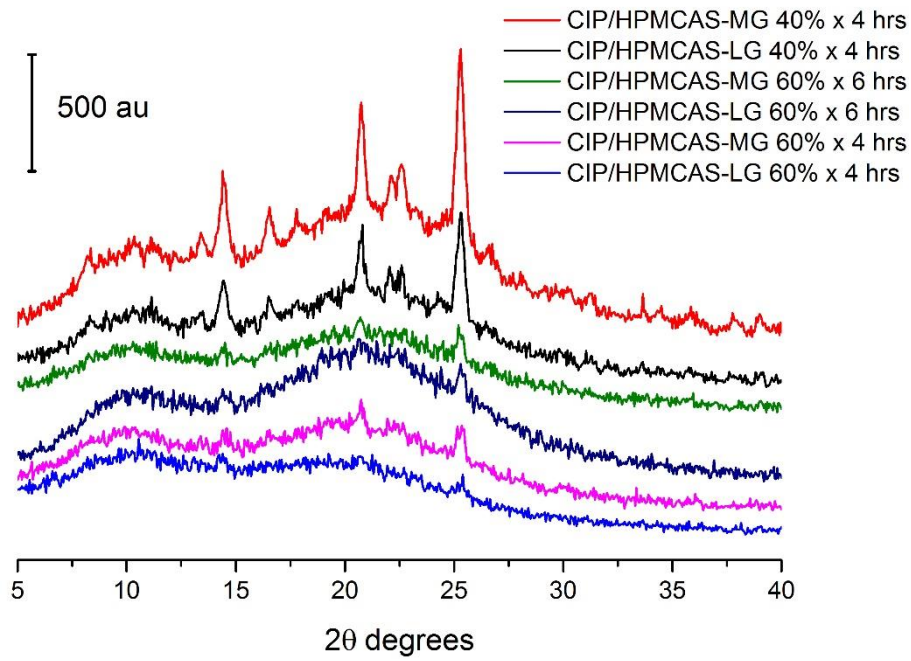

Figure SI.4. PXRD analysis of solid dispersions formed by milling CIP with 40–60% (w/w) HPMCAS-LG and HPMCAS-MG for 4 or 6 hours at room temperature.

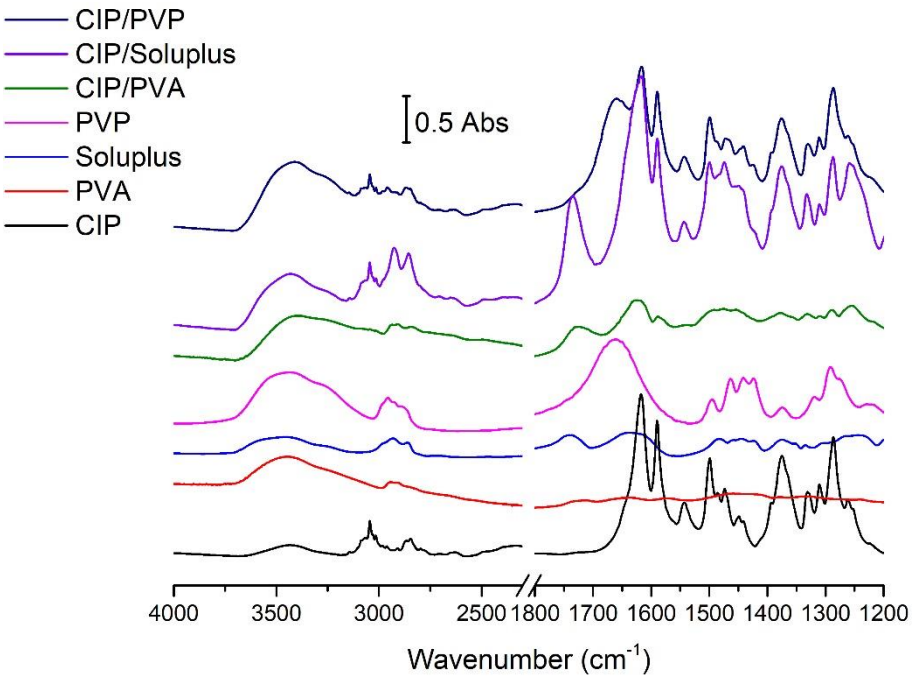

Figure SI.5. FTIR analysis of partially crystalline solid dispersions formed by milling CIP with 40% (w/w) PVP, Soluplus or PVA.

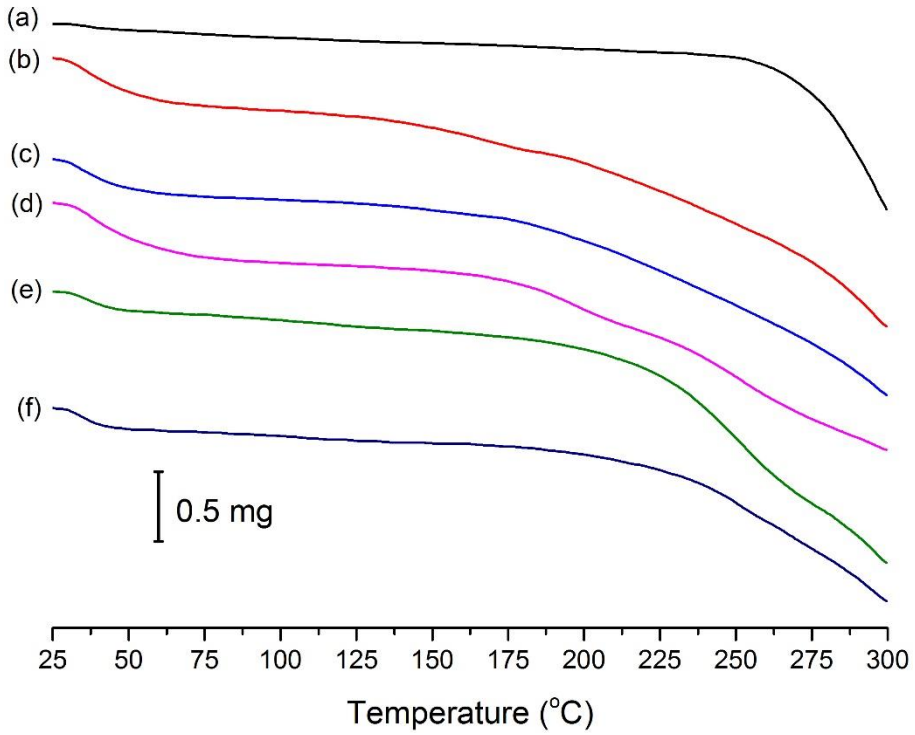

Figure SI.6. TGA analysis of (a) crystalline CIP, and ASDs containing (b) Eudragit L100 40% (w/w) (c) Eudragit L100-55 40% (w/w) (d) Carbopol 40% (w/w) (e) HPMCAS-LG 60% (w/w) and (f) HPMCAS-MG 60% (w/w).

Eudragit L100:

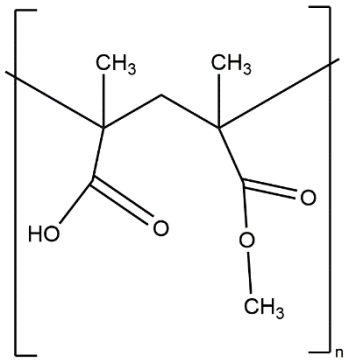

Eudragit L100-55:

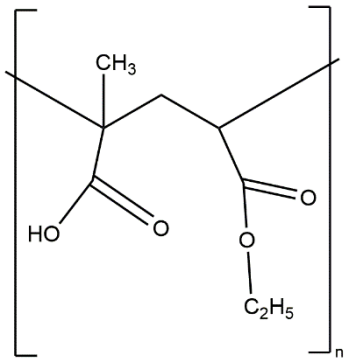

Carbopol:

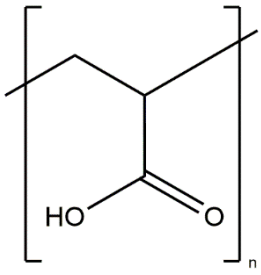

HPMCAS:

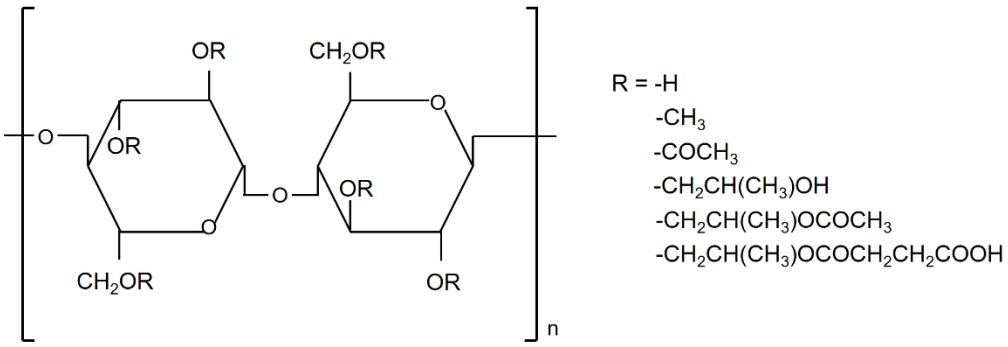

Figure SI.7. Chemical structures of polymers used in this study. The different grades of HPMCAS differ in their substituent content.

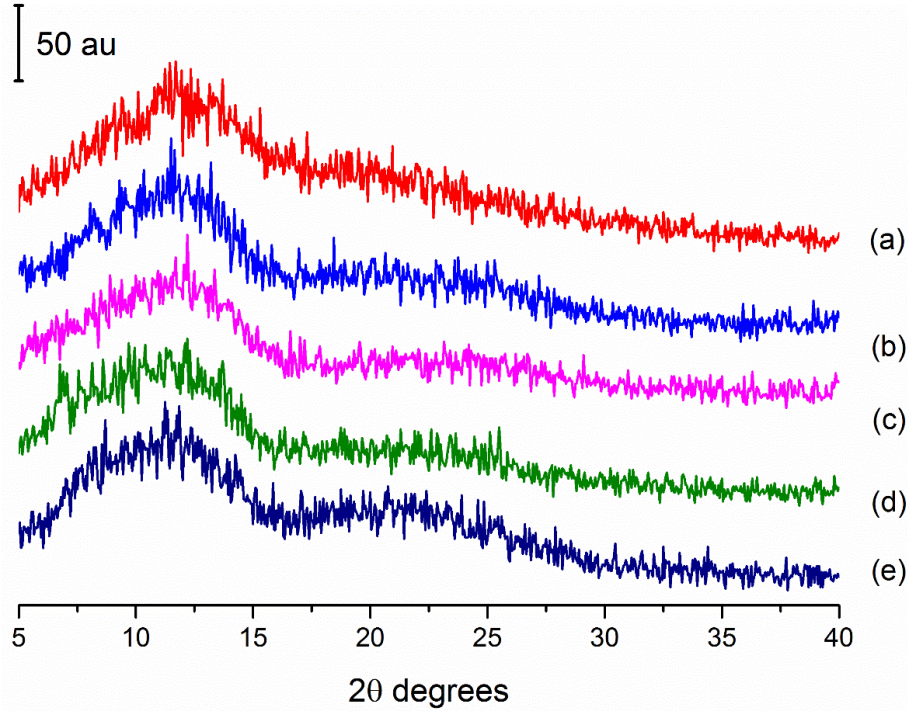

Figure SI.8. PXRD following DVS analysis of CIP ASDs containing (a) Eudragit L100 40% (w/w) (b) Eudragit L100-55 40% (w/w) (c) Carbopol 40% (w/w) (d) HPMCAS-LG 60% (w/w) and (e) HPMCAS-MG 60% (w/w).

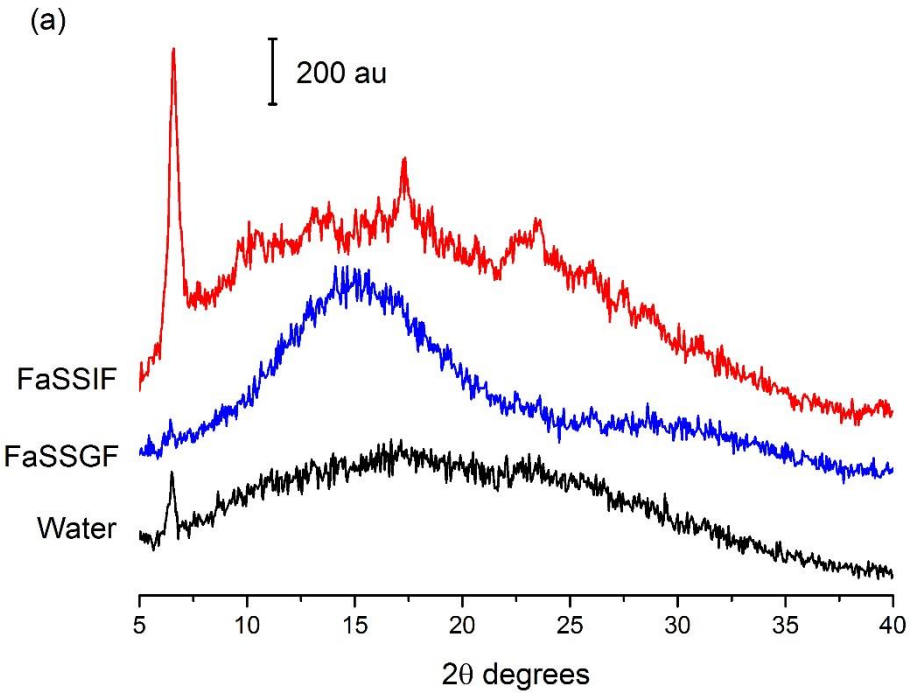
(a)
200 au
FaSSIF
FaSSGF
Water
5
10
15
20
25
30
35
40
2θ degrees

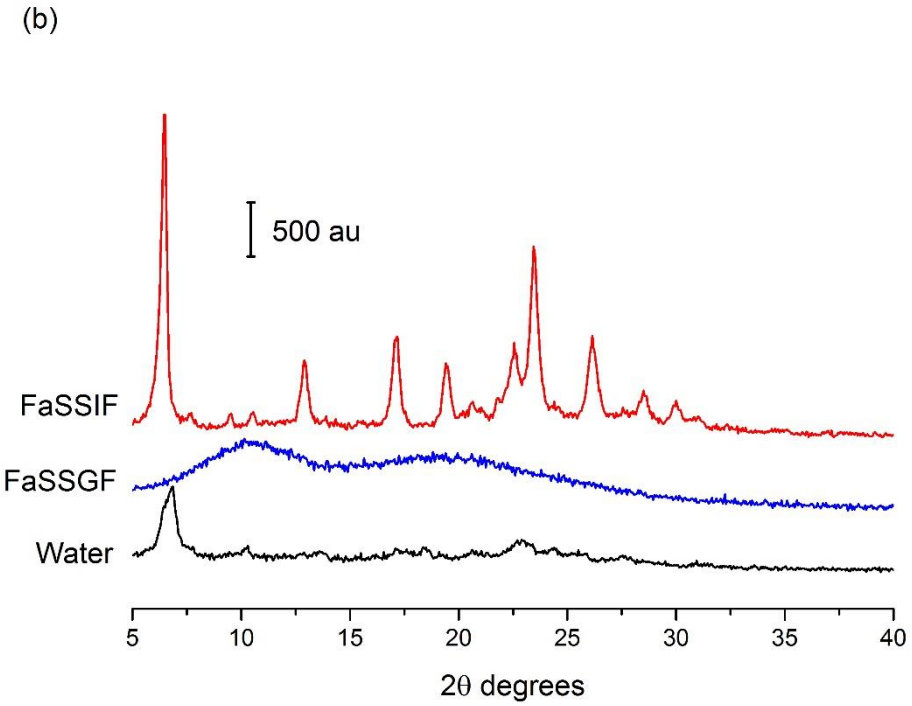
(b)
500 au
FaSSIF
FaSSGF
Water
5
10
15
20
25
30
35
40
2θ degrees

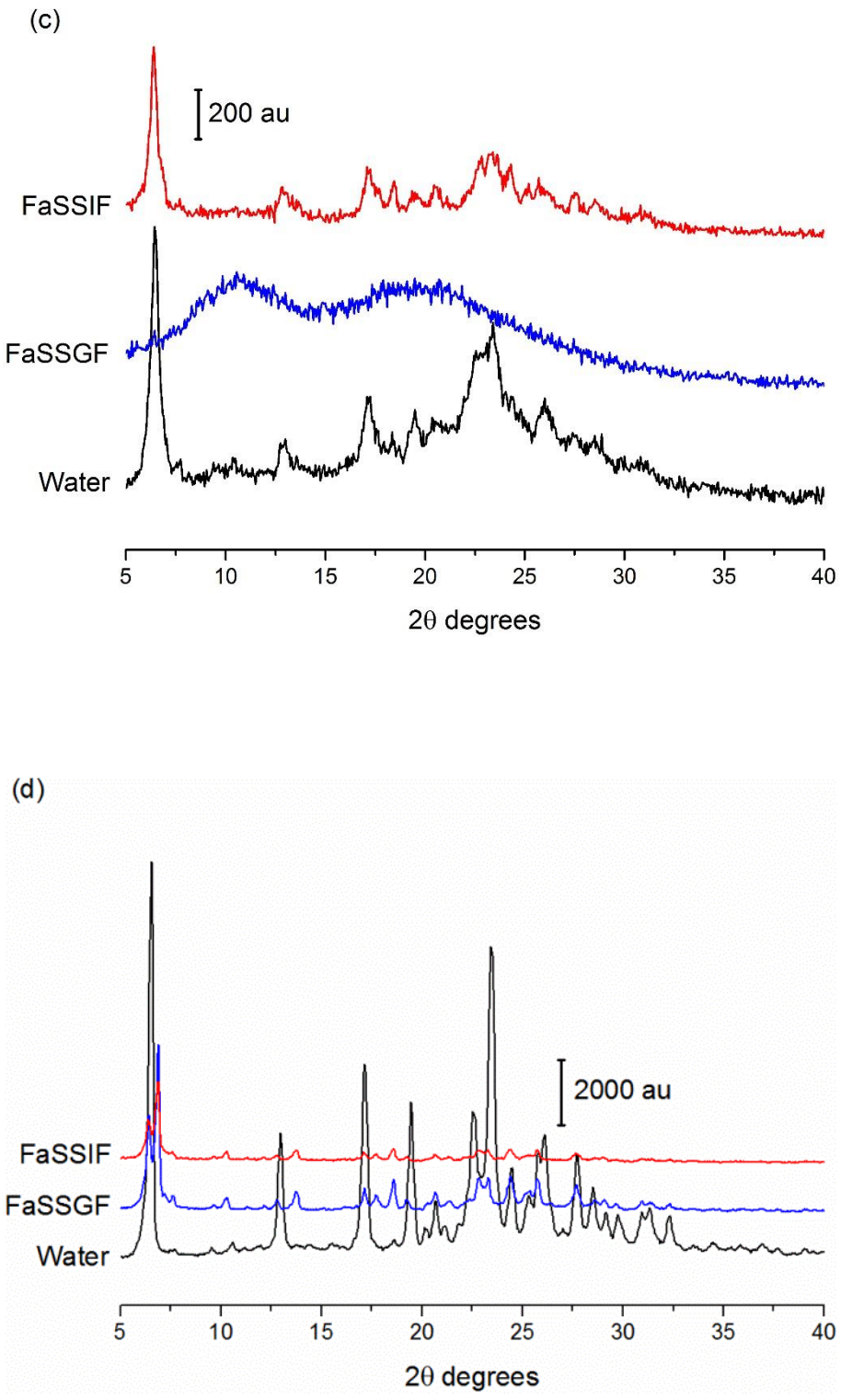

Figure SI.9. PXRD analysis following solubility studies of (a) CIP/Eudragit L100 (b) CIP/HPMCAS-LG (c) CIP/HPMCAS-MG and (d) CIP.

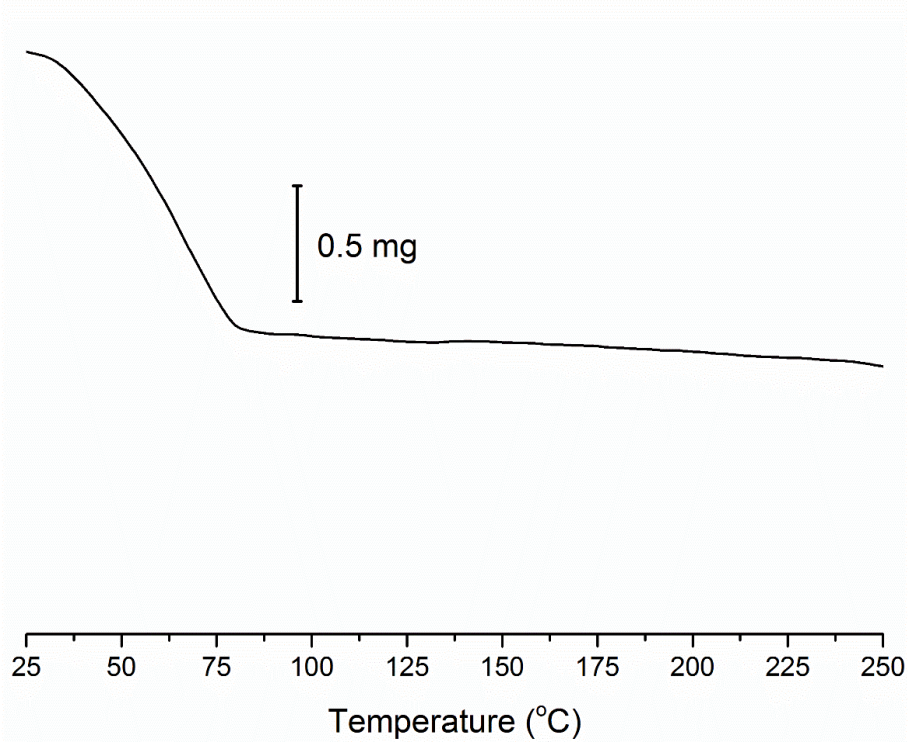

Figure SI.10. TGA of hydrate obtained following solubility studies of crystalline CIP in water.